



# Superdiffusive Transport in Space and Astrophysical Plasmas

**Silvia Perri**

[silvia.perri@fis.unical.it](mailto:silvia.perri@fis.unical.it)

Dipartimento di Fisica Università della Calabria, Rende, Italy

in collaboration with: *G. Zimbardo, E. Amato, F. Effenberger, H. Fichtner, and G. Prete*

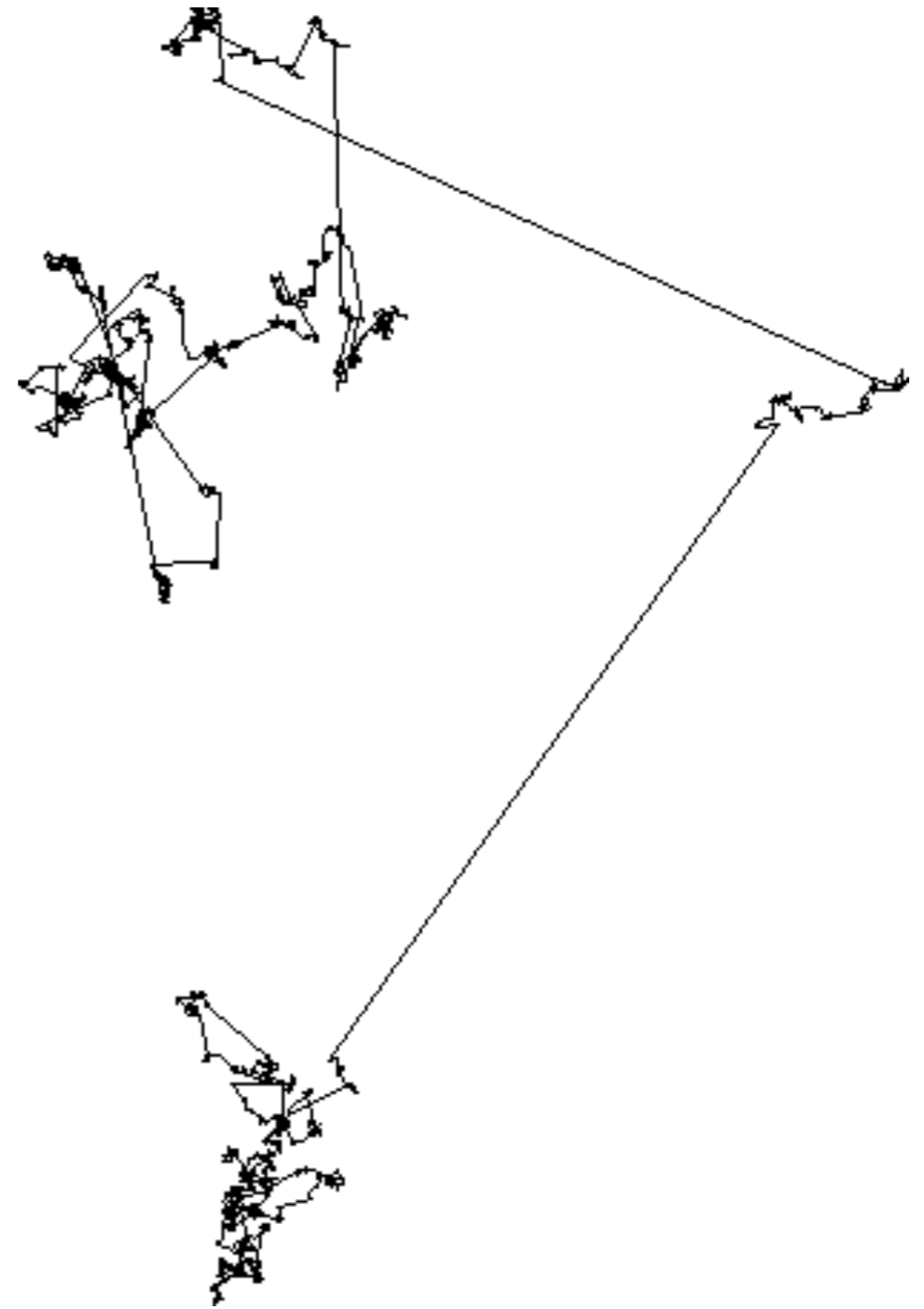
# Outline

- An overview of anomalous transport in physical systems;
- Energetic particles in the interplanetary space;
- How to infer transport properties from in-situ measurements of particle fluxes;
- Superdiffusion upstream of interplanetary shock waves and superdiffusive shock acceleration;
- From in-situ to remote observations: superdiffusion in astrophysical plasmas;
- New perspectives with Parker Solar Probe and Solar Orbiter

## Normal (Gaussian)



## Anomalous (Lèvy random walk)



An increasing number of natural phenomena do not fit into the relatively simple description of diffusion developed by Einstein a century ago

# Anomalous diffusion spreads its wings

Joseph Klafter and Igor M Sokolov

AS ALL of us are no doubt aware, this year has been declared “world year of physics” to celebrate the three remarkable breakthroughs made by Albert Einstein in 1905. However, it is not so well known that Einstein’s work on Brownian motion – the random motion of tiny particles first observed and investigated by the botanist Robert Brown in 1827 – has been cited more times in the scientific literature than his more famous papers on special relativity and the quantum nature of light. In a series of publications that included his doctoral thesis, Einstein derived an equation for Brownian motion from microscopic principles – a feat that ultimately enabled Jean Perrin and others to prove the existence of atoms (see *Physics World* January pp 19–22).

Einstein was not the only person thinking about this type of problem. The 27 July 1905 issue of *Nature* contained a letter with the title “The problem of the random walk”, in which the British statistician Karl Pearson proposed the following: “A man starts from the point  $O$  and walks  $l$  yards in a straight line; he then turns through any angle whatever and walks another  $l$  yards in a second straight line. He repeats this process  $n$  times.



Strange behaviour – albatrosses fly by the rules of anomalous diffusion.

of his work on Brownian motion. He did this by assuming that the direction of motion of a particle gets “forgotten” after a certain time, and that the mean-squared displacement during this time is finite. When Einstein combined the diffusion equation with the Boltzmann distribution for a system in thermal equilibrium, he was able to predict the properties of the unceasing motion of Brownian particles in terms of collisions with surrounding liquid molecules. This was the breakthrough that ultimately led to scientists believing in the reality of atoms.

in living organisms. In 1855 Fick published the famous diffusion equation, which, when written in terms of probability, is  $\partial p/\partial t = D\partial^2 p/\partial x^2$ , where  $p$  gives the probability of finding an object at a certain position  $x$ , at a time  $t$ , and  $D$  is the diffusion coefficient. Fick went on to show that the mean-squared displacement of an object undergoing diffusion is  $2Dt$ .

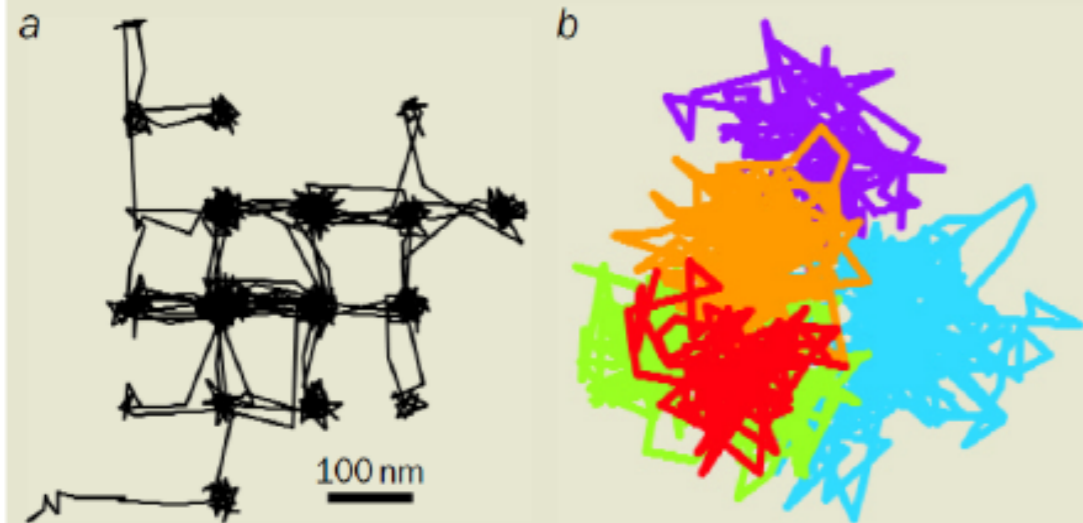
However, Fick’s approach was purely phenomenological, based on an analogy with Fourier’s heat equation – it took Einstein to derive the diffusion equation from first principles as part

of his work on Brownian motion. He did this by assuming that the direction of motion of a particle gets “forgotten” after a certain time, and that the mean-squared displacement during this time is finite. When Einstein combined the diffusion equation with the Boltzmann distribution for a system in thermal equilibrium, he was able to predict the properties of the unceasing motion of Brownian particles in terms of collisions with surrounding liquid molecules. This was the breakthrough that ultimately led to scientists believing in the reality of atoms.

# Observations of anomalous transport

Klafter and Sokolov, 2005

## 3 Subdiffusion in cells



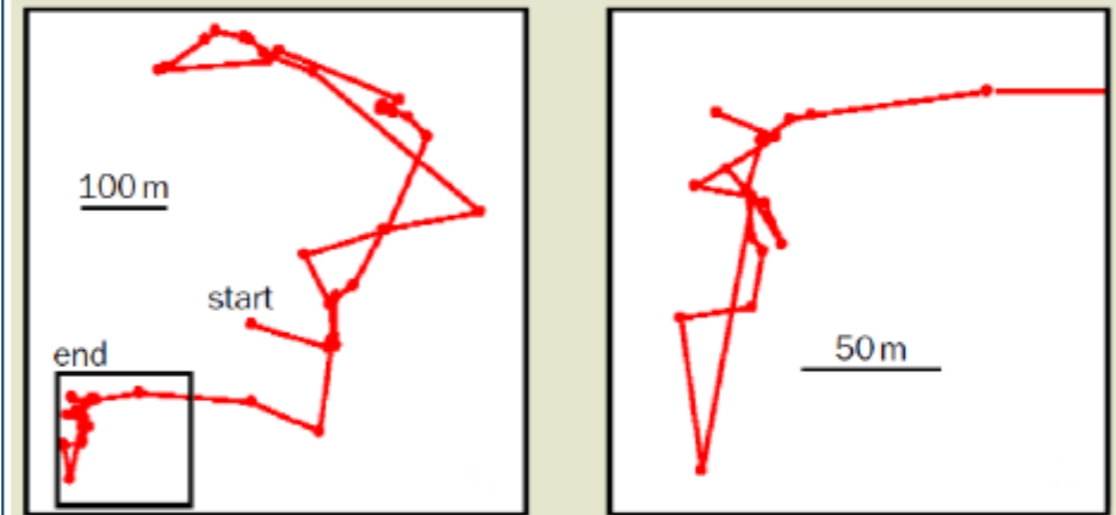
Researchers have found that the way proteins diffuse across cell membranes can be described by anomalous diffusion that is slower than the normal case. (a) This is a simulation of such a random walk, which shows a 2 ms timeframe over which a protein "hops" between 120 nm<sup>2</sup> compartments thought to be formed by the cell's cytoskeleton. (b) The experimental trajectories of proteins in the plasma membrane of a live cell (shown in a 0.025 ms timeframe) provide evidence for this trapping nature,

$$\langle \Delta r^2 \rangle = 2D_{\alpha} t^{\alpha}$$

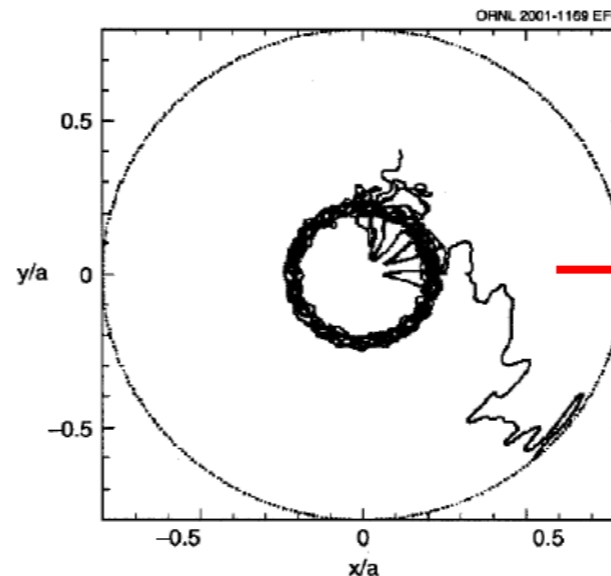
Subdiffusion  
 $\alpha < 1$

Superdiffusion  
 $\alpha > 1$

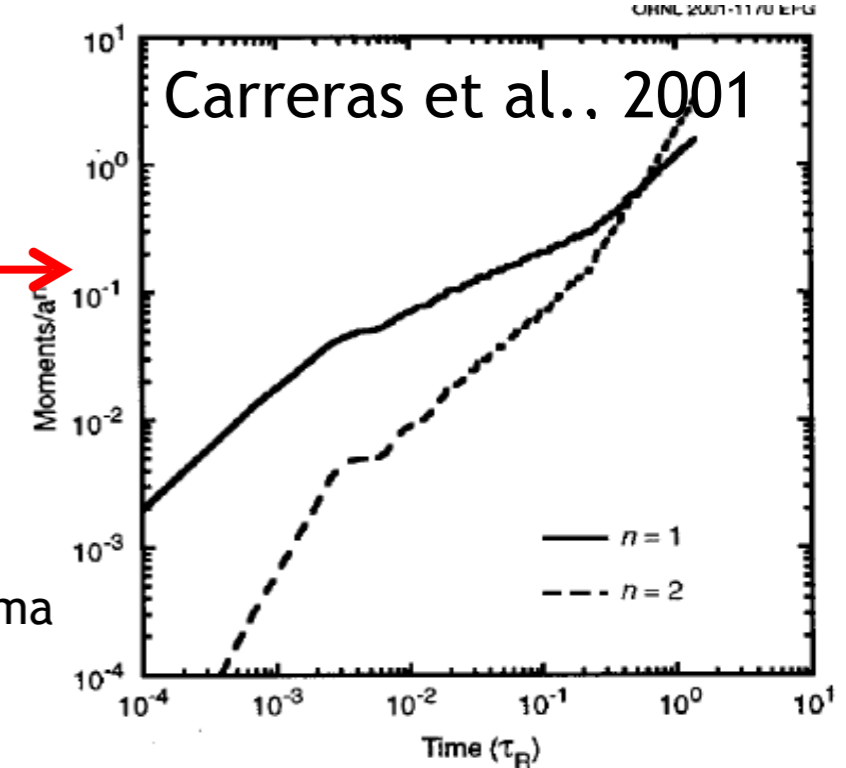
## 4 Superdiffusion in monkey behaviour



The typical trajectories of spider monkeys in the forest of the Mexican Yucatan peninsula display steps with variable lengths, which correspond to a diffusive process that is faster than that of normal diffusion. An example of such a trajectory is shown on the left. A magnified part of it is shown on the right; this image looks qualitatively similar to the larger-scale trajectory, which is an important property of Lévy walks. Similar behaviour is found in the



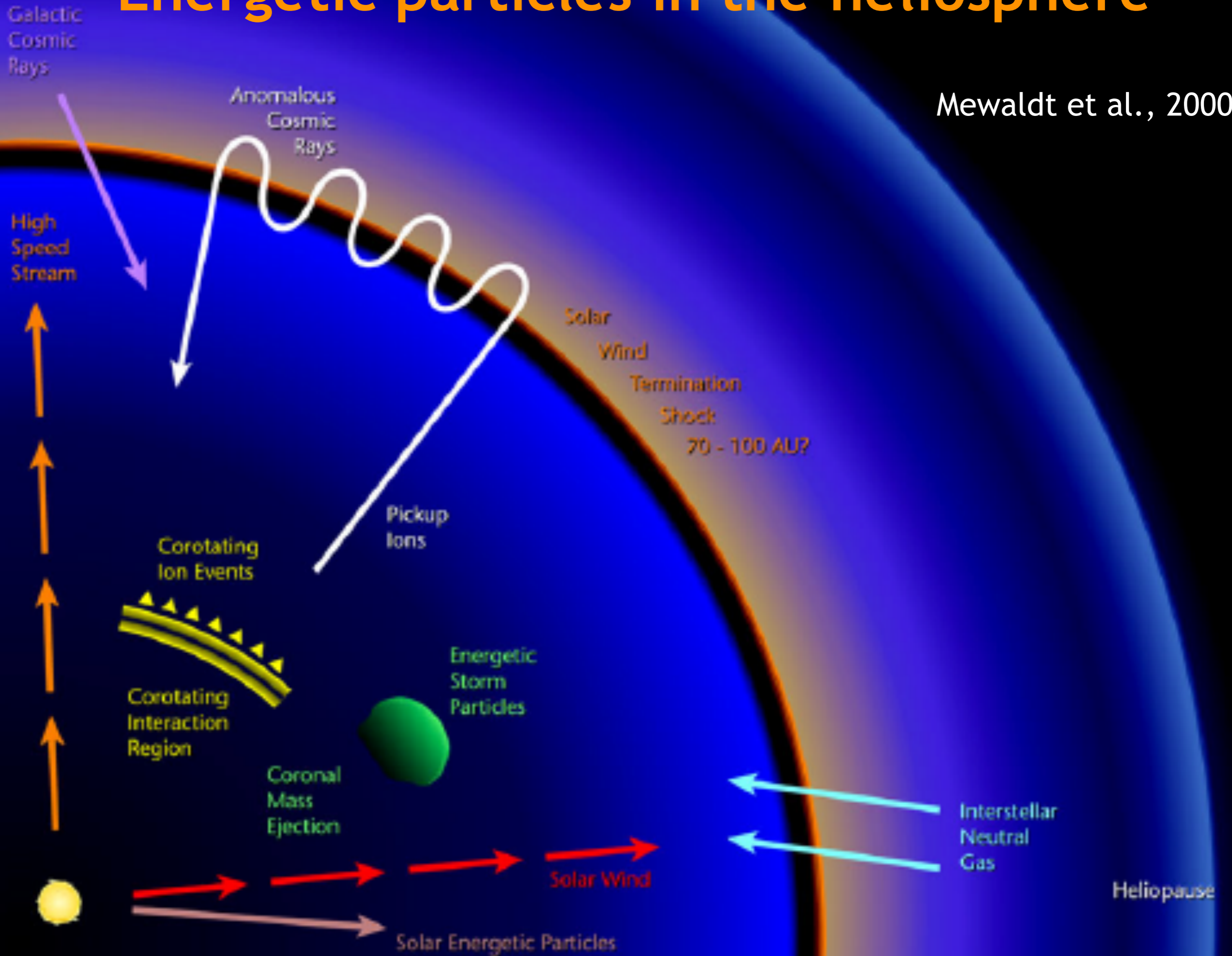
Particle trajectories in a cylindrical plasma model

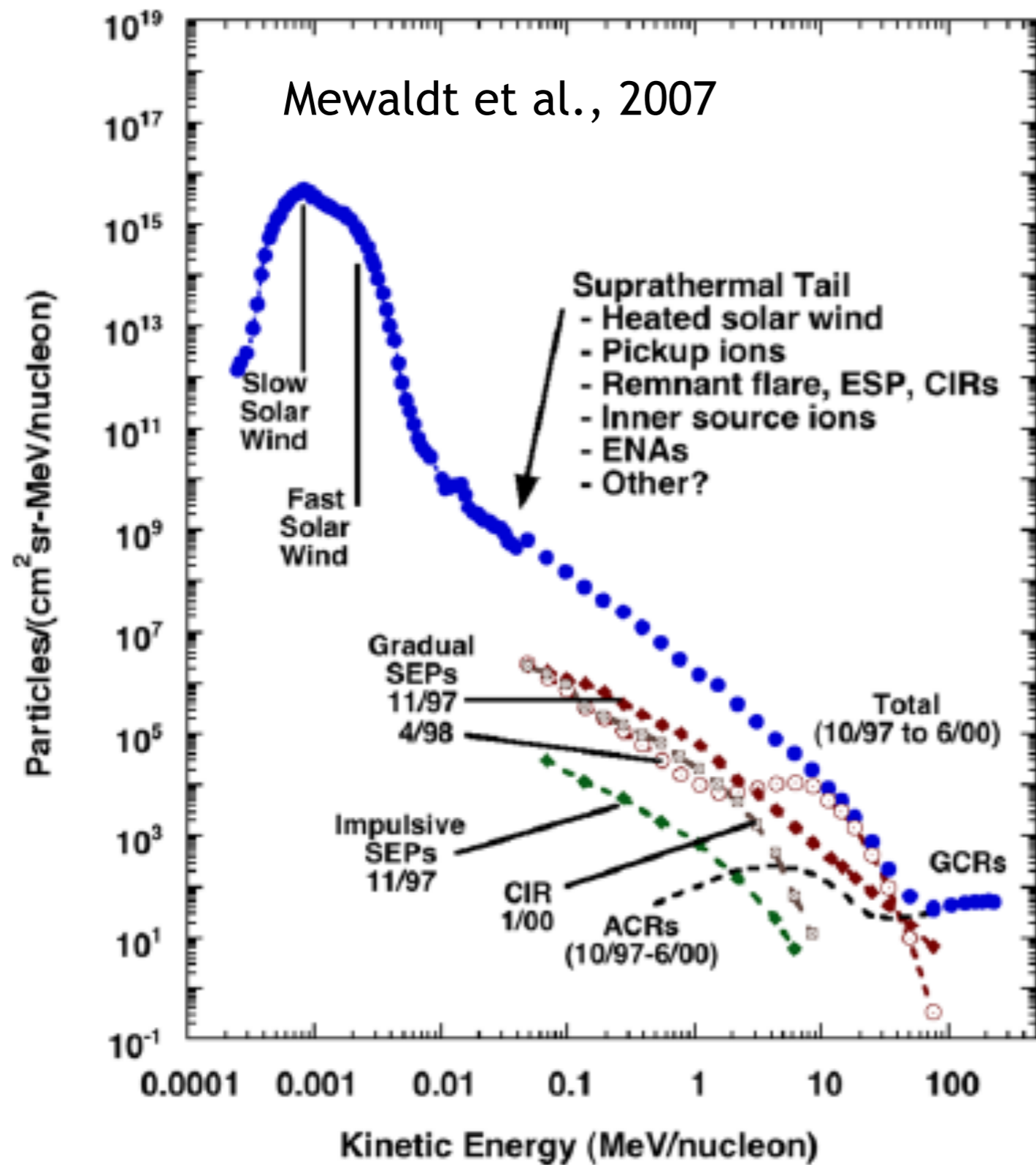


$$\langle [r(t) - r(0)]^n \rangle = D_0 t^{n\nu(n)}$$

# Energetic particles in the heliosphere

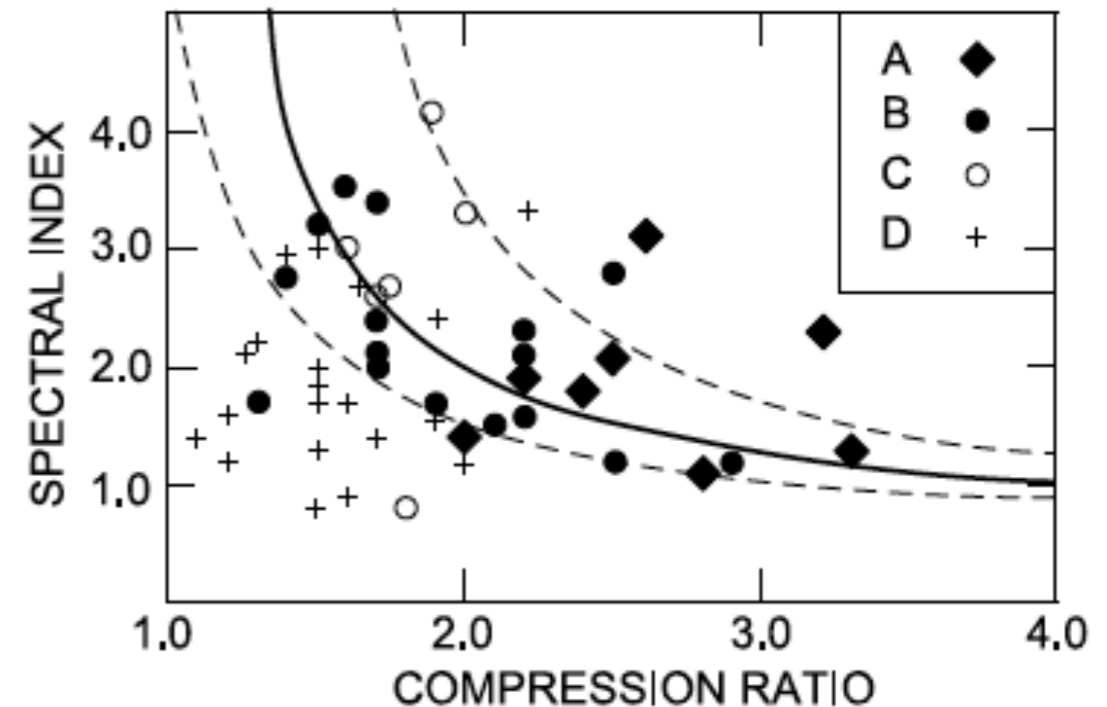
Mewaldt et al., 2000





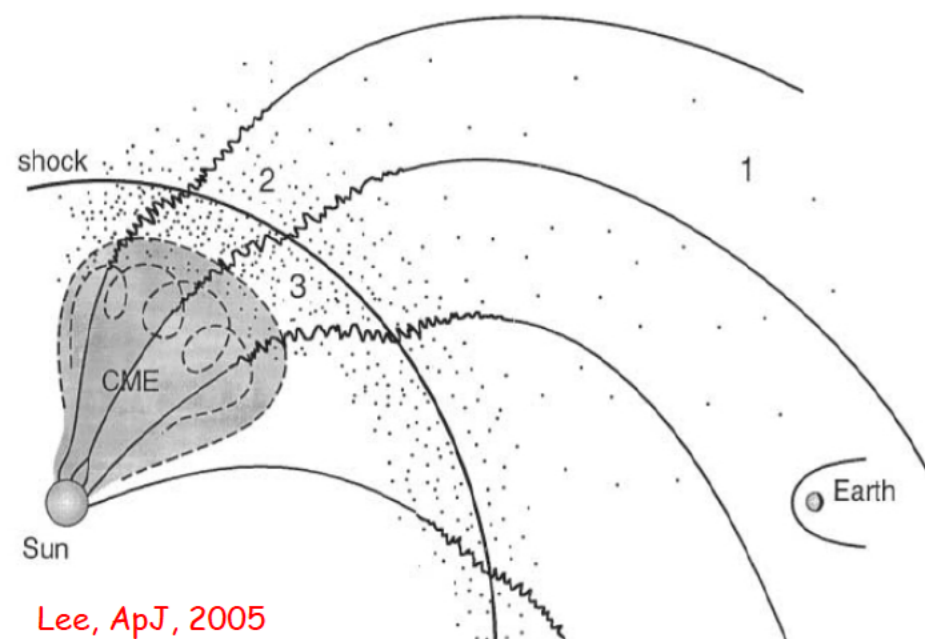
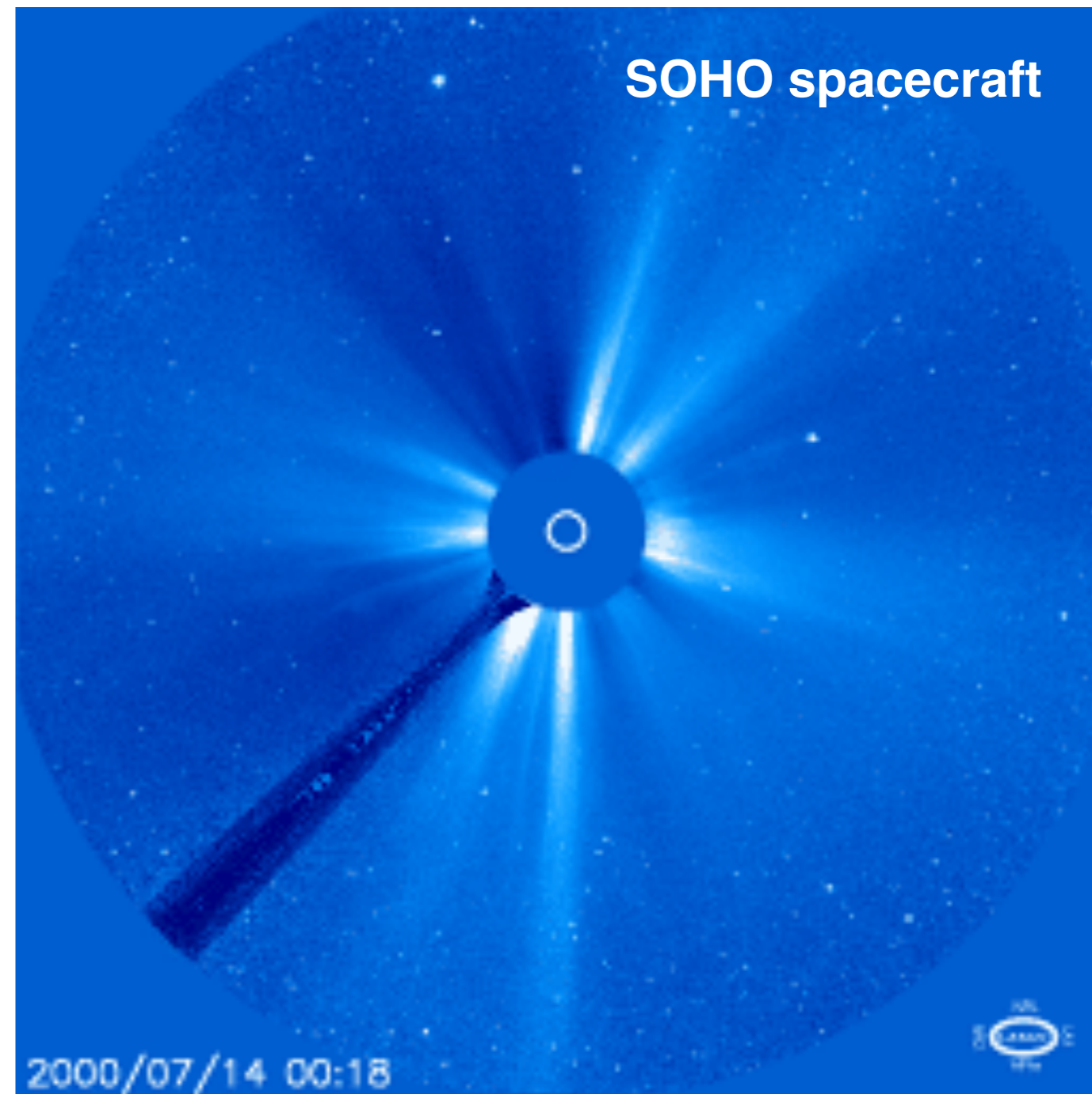
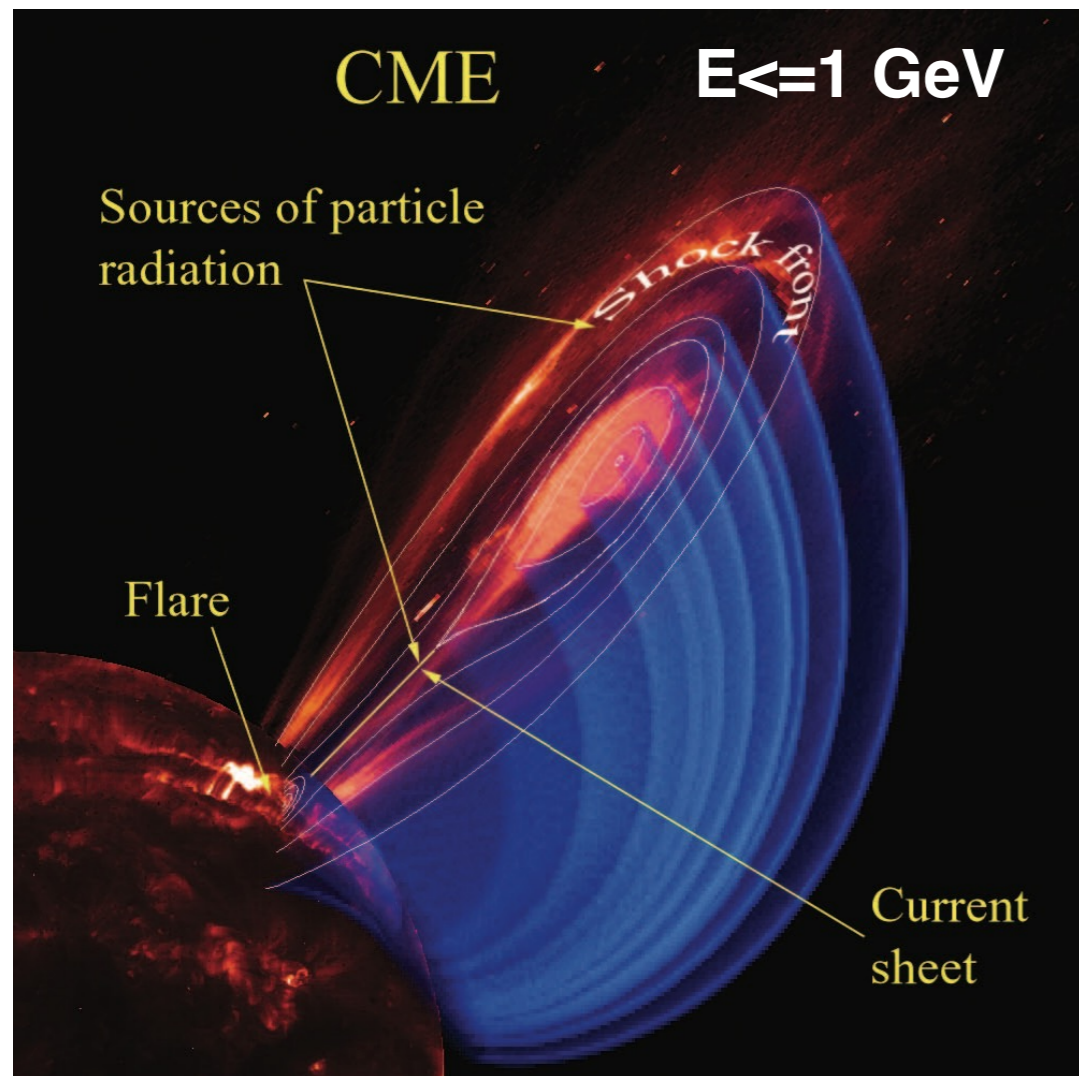
The particle energy spectral index varies a lot in different events and there is a tendency to deviate from the diffusive shock acceleration prediction

van Nes et al., 1984



The energy spectrum varies with the solar cycle.

# Solar energetic particles



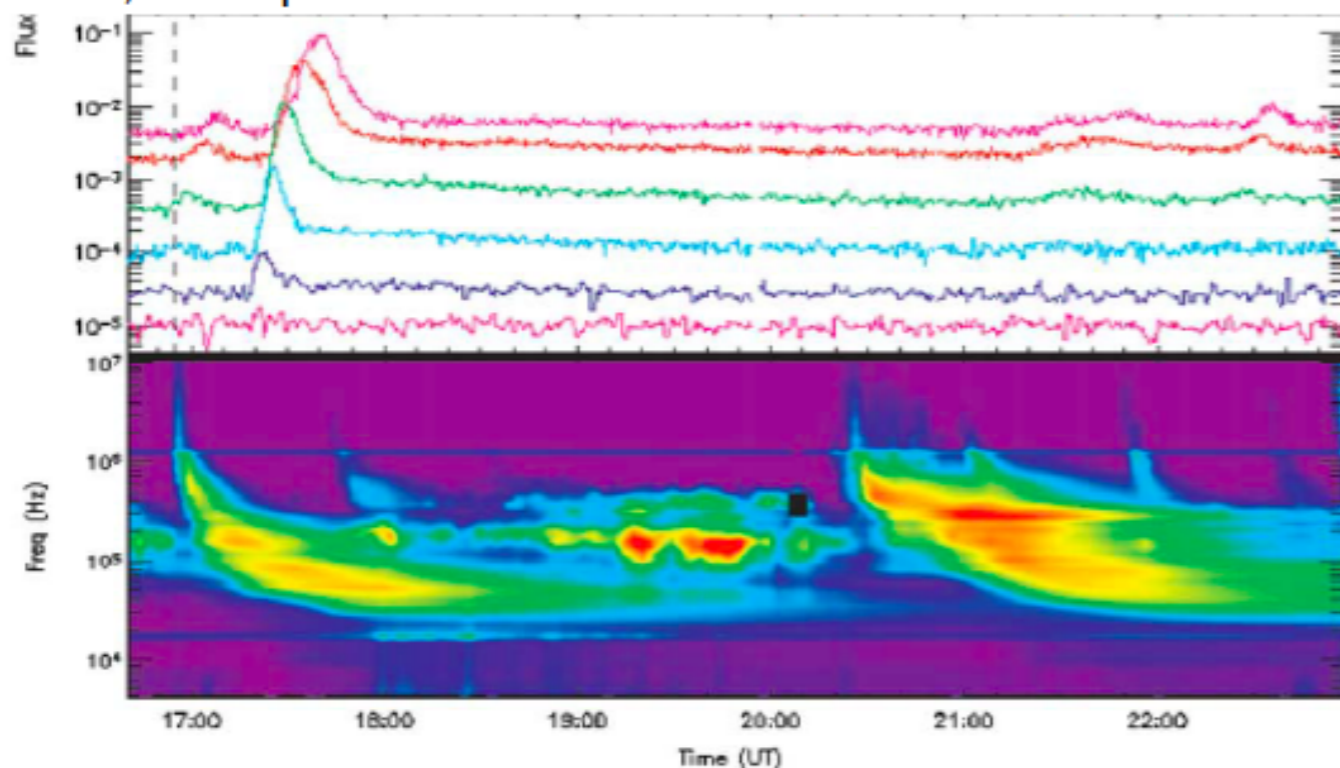
Lee, ApJ, 2005

Predicting their arrival to the Earth is crucial for protecting astronauts, scientific and commercial satellites



# Indication of anomalous transport in the interplanetary space

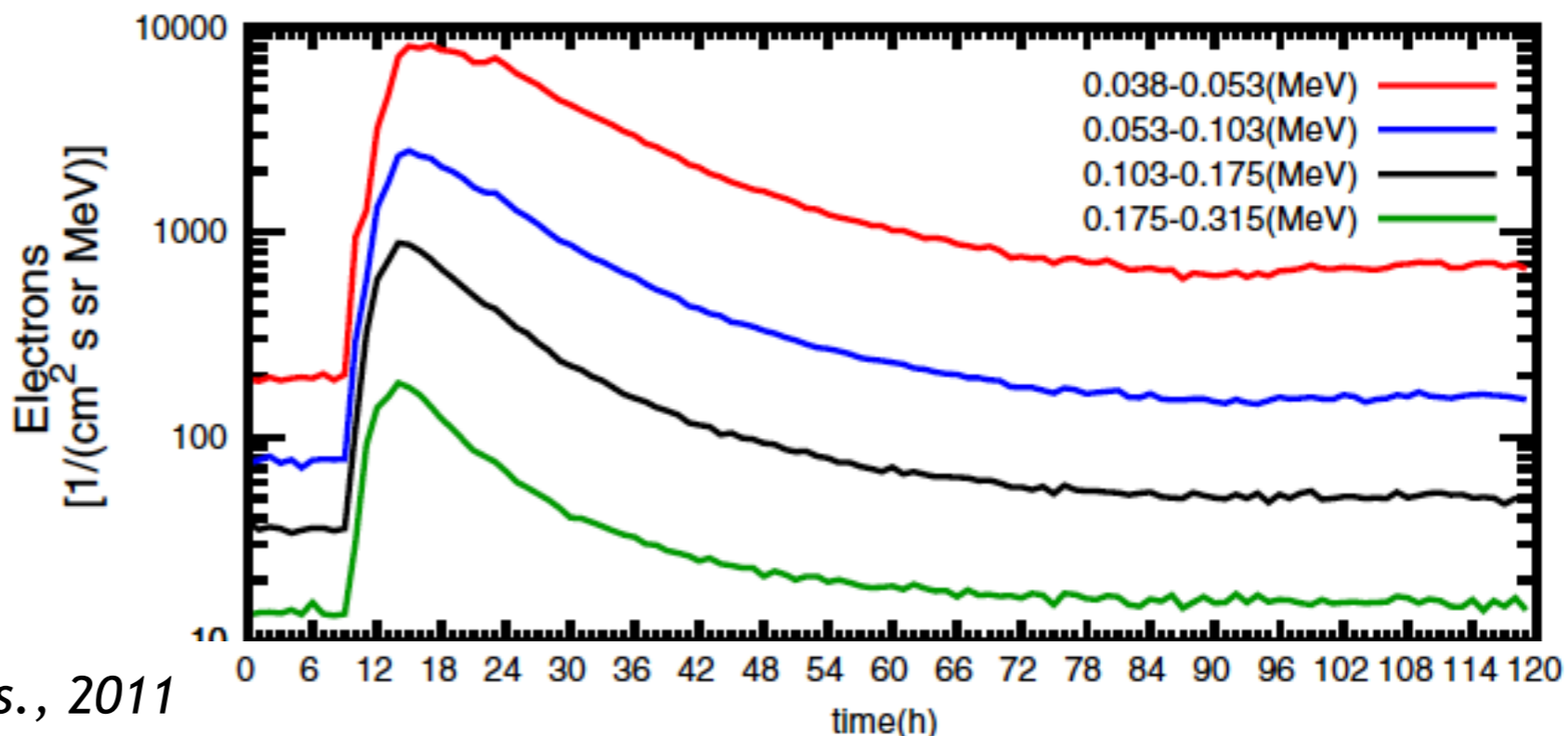
Lin, Adv. Space Res. 2005



Scatter free  
impulsive  
electrons  
events from  
WIND

available flare energy into fast electrons. Non-relativistic electrons exhibit a wide variety of propagation modes in the interplanetary medium, ranging from diffusive to essentially scatter-free. This

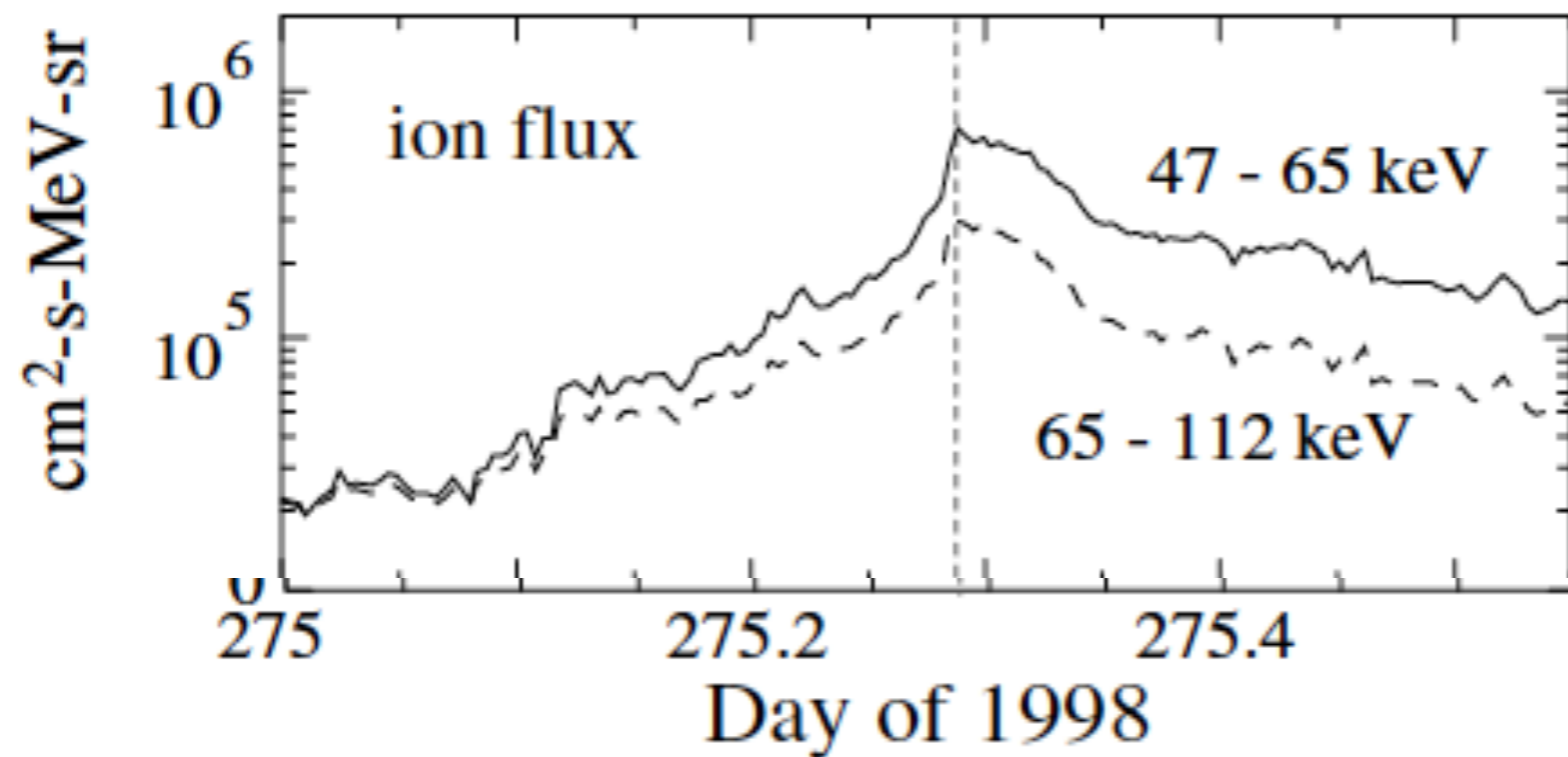
Scattering leads to the formation of a gradual tail in the time particle fluxes



Trotta and Zimbardo, Astron. Astrophys., 2011

# Acceleration and transport at interplanetary shocks

From Giacalone, ApJ 2012



Energetic particle profiles tend to peak at the shock

The diffusive shock acceleration theory (DSA) predicts an exponential rise upstream (in the case of spatially constant diffusion coefficient) and a flat, constant, profile downstream

For planar shocks

$$f(x, p) = Ap^{-3r/(r-1)} H(p - p_0) \begin{cases} \exp(U_1 x / \kappa_{xx}) & x \leq 0 & \text{upstream} \\ 1 & x > 0, & \text{downstream} \end{cases}$$

**These predicted profiles are not always observed**

# Superdiffusive transport for particle accelerated at shocks

Assuming particles accelerated by an infinite planar shock (1D geometry), we can reconstruct the particle profiles using a probabilistic approach (*propagator*):

$$n(x, E, t) = \int P(x - x', t - t') S_{sh}(x', E, t') dx' dt'$$

Particle injected at the shock

$$S_{sh}(x', E, t') = \Phi_0(E) \delta(x' - V_{sh} t')$$

$$P(x - x', t - t') = b \frac{t - t'}{(x - x')^\mu}$$

$$n(0, E, t) \propto \frac{1}{(-t)^\beta}$$

$$\beta = \mu - 2$$

$$2 < \mu < 3$$

$P(x - x', t - t')$  describes an **anomalous transport** process and goes to zero for  $x - x' > v(t - t')$  - far from the source, with  $v$  the particle velocity (*Zumofen and Klafter, 1993*)

The mean square displacement is related to the exponent of the power law via the relation (*Zumofen and Klafter, 1993*)

$$\langle x^2(t) \rangle = 2D_\alpha t^\alpha, \text{ with } \alpha = 4 - \mu = 2 - \beta, \quad 2 < \mu < 3, \quad 0 < \beta < 1$$

Normal diffusion

$$\langle x(t)^2 \rangle = 2Dt$$

$$P(x, t) = \frac{1}{\sqrt{2\pi Dt}} \exp\left[-\frac{x^2}{2Dt}\right]$$

Energetic particle profile from diffusive shock acceleration (DSA)  
(*Lee and Fisk, 1982*)

$$n(x, E) \propto e^{-V|x|/D}$$

Superdiffusion

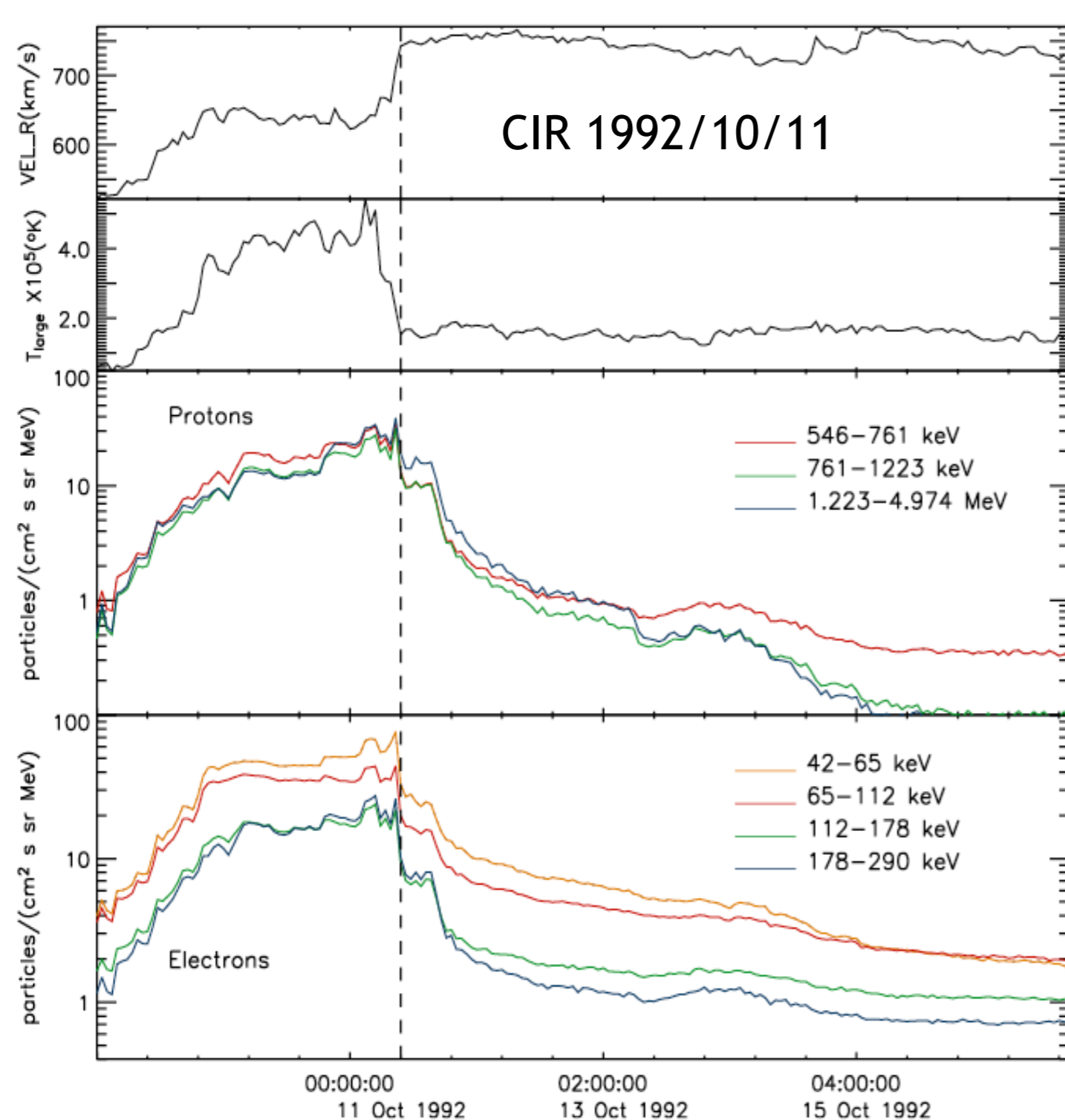
$$\langle x(t)^2 \rangle = 2D_\alpha t^\alpha \quad \alpha > 1$$

$$P(x, t) \approx \frac{t}{x^\mu} \quad \alpha = 4 - \mu$$

Energetic particle profile  
(*Perri and Zimbardo, 2008*)

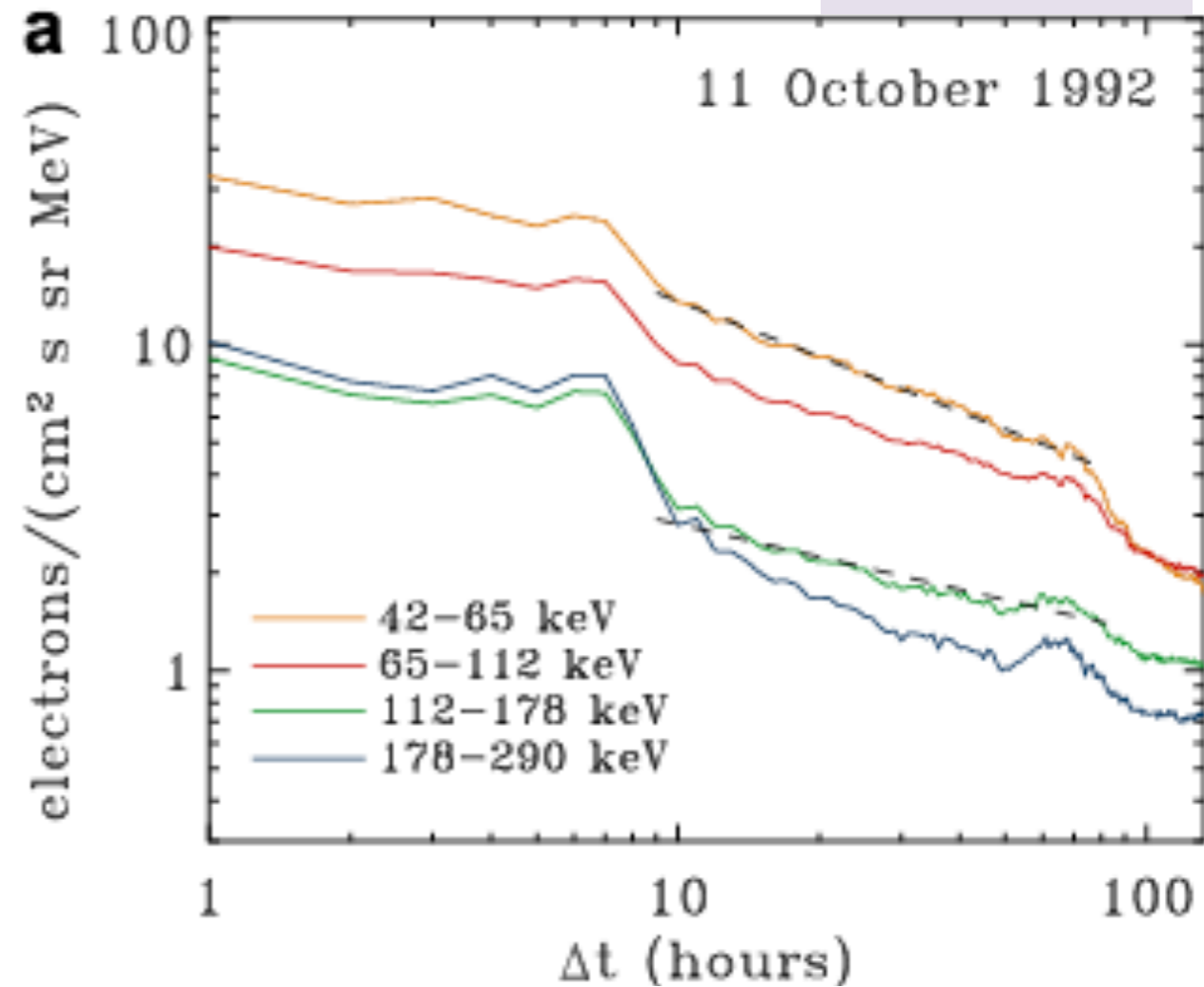
$$n(x, E) \propto |x|^{-\beta} \quad \beta = \mu - 2$$

# Evidence for superdiffusive transport from particle profiles



$$n(\Delta t, E) \propto |\Delta t|^{-\beta}$$

$|x| = V_{sh} \Delta t$



$$\Delta t = |t - t_{sh}|$$

$$\langle \Delta x^2(t) \rangle \propto t^{2-\beta}$$

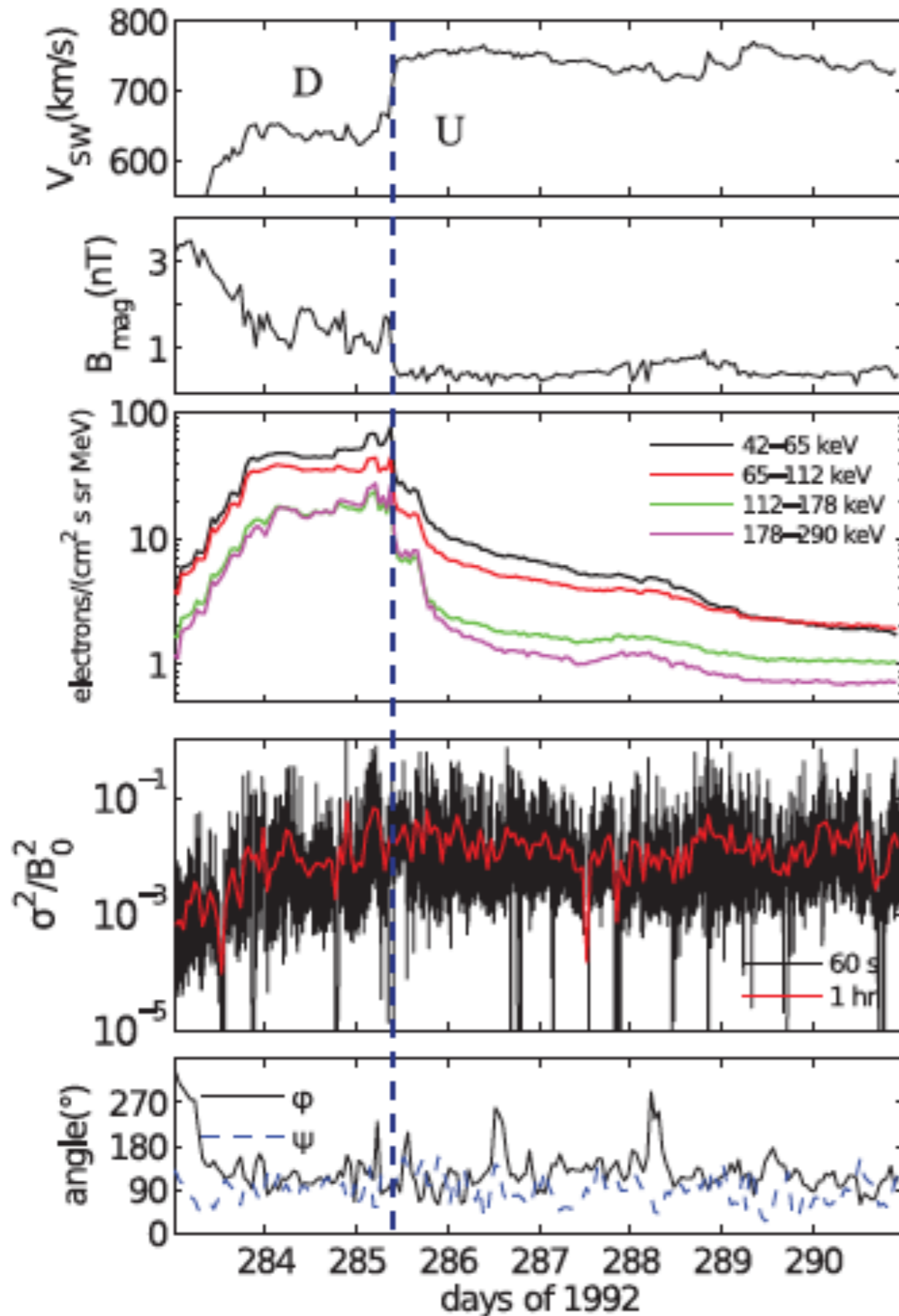
$$2 - \beta \in [1.44, 1.70]$$

## Particle scattering frequency

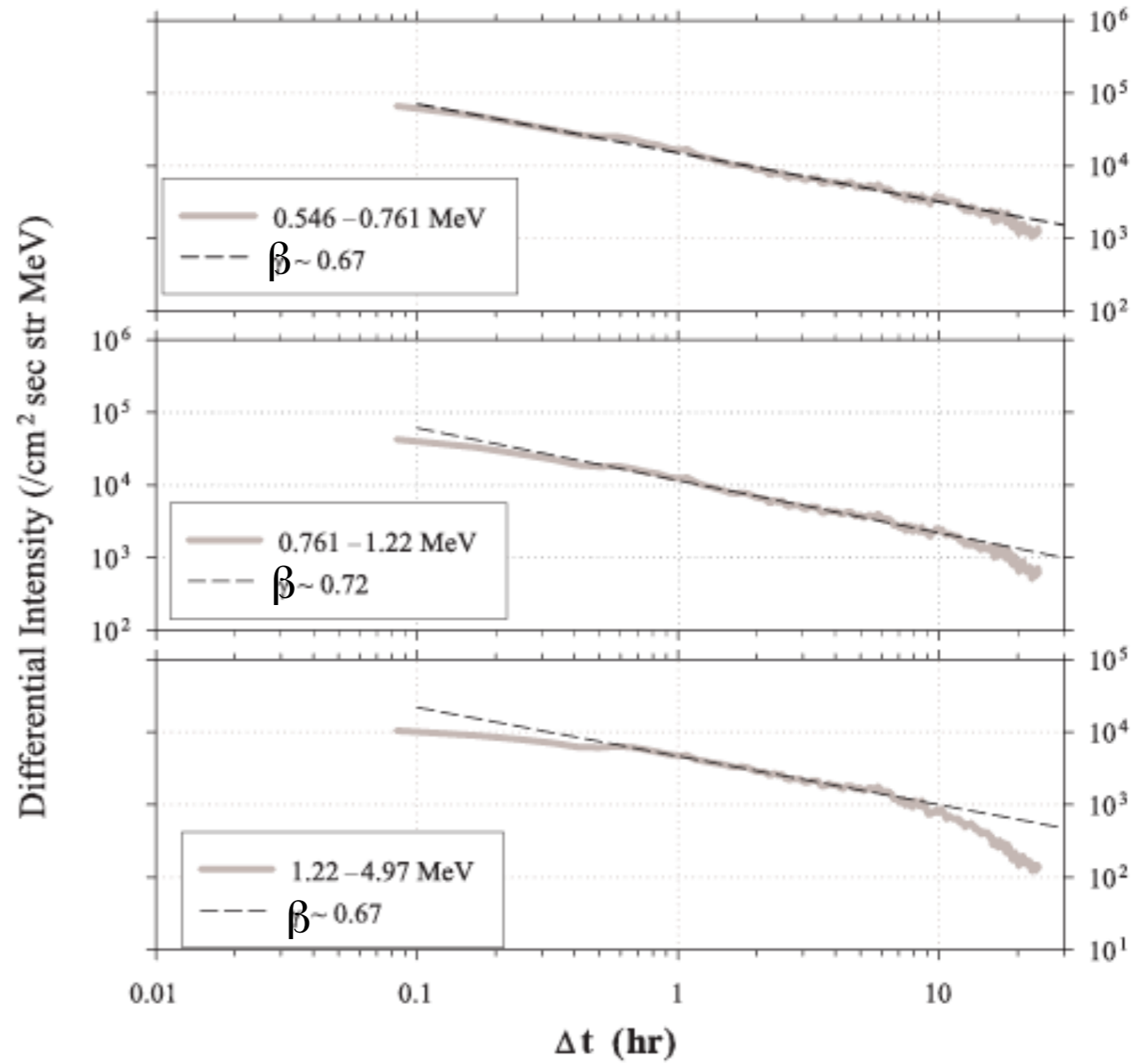
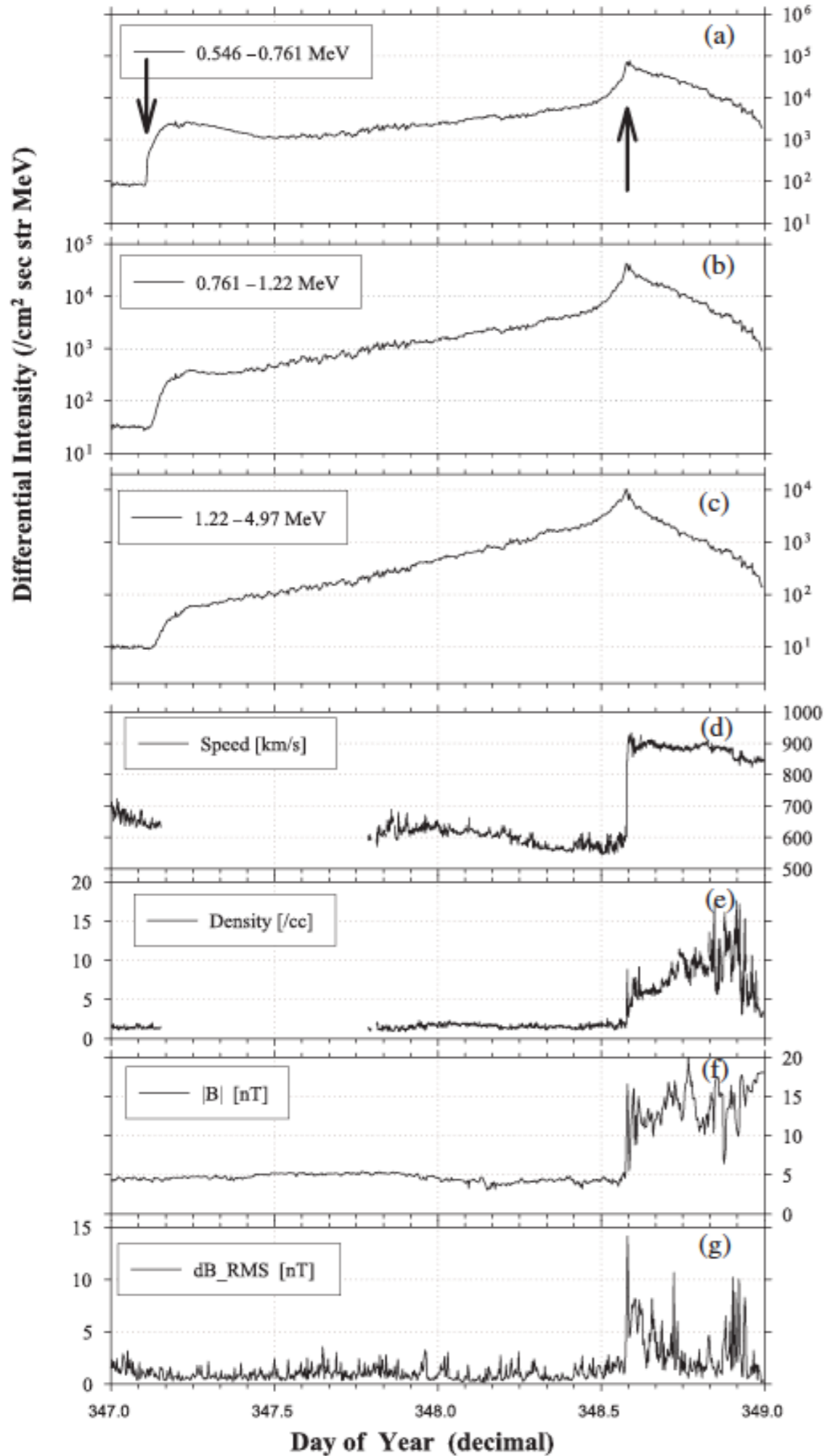
$$\nu_s = \frac{\pi}{4} \Omega \left\langle \left( \frac{\delta B_{\text{res}}}{B_0} \right)^2 \right\rangle$$

$$D = v \lambda_{\text{mfp}} / 3, \quad \text{spatial diffusion coefficient}$$

$$\lambda_{\text{mfp}} = v / \nu_s$$



The analysis of magnetic field variances computed at the scale of the energetic particles shows that the level of magnetic field fluctuation is almost constant upstream of the shock front, implying a spatially/time constant diffusion coefficient

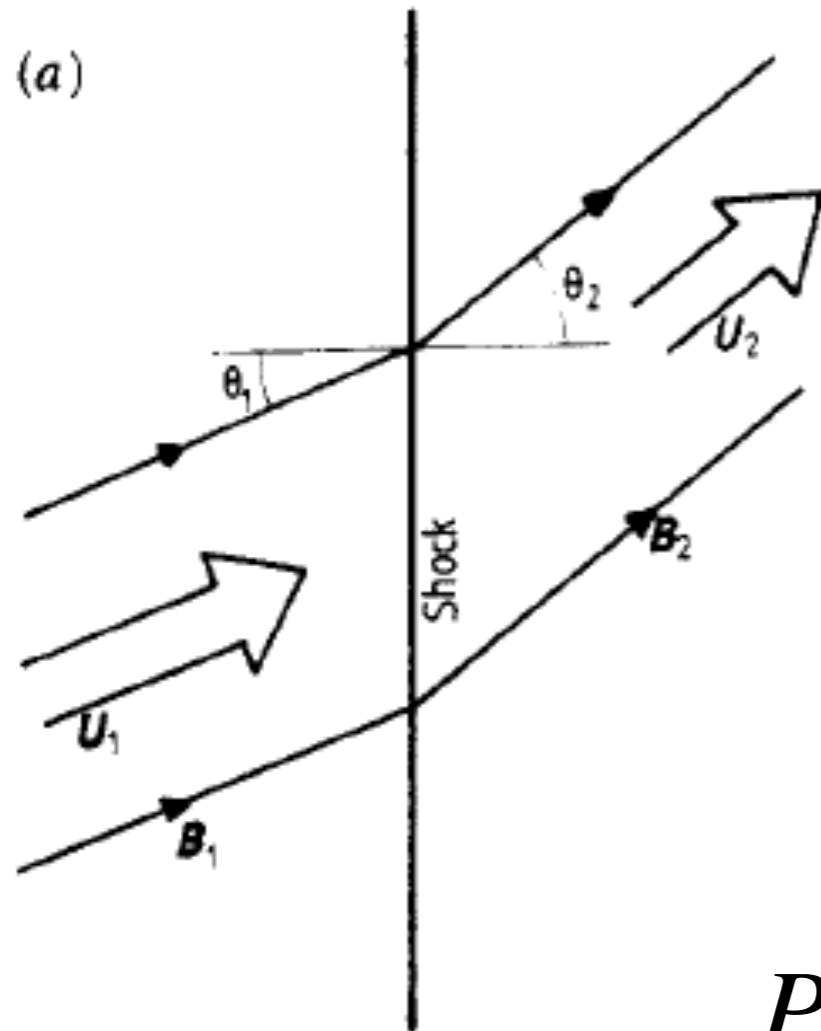


Ions accelerated at a coronal mass ejection driven shock

$$\beta < 1 \quad \alpha > 1$$

# First order Fermi acceleration

Drury, Rep. Prog. Phys. 1983



$$\Delta E = \xi E_0$$

Energy gained by a particle after  $n$  encounters with the shock

$$\left\langle \frac{\Delta E}{E} \right\rangle = \frac{4}{3} \frac{V_1 - V_2}{v}$$

The probability for a particle to leave the acceleration region is (Geisser 1990)

$$P_{esc} = \frac{\Phi_2}{\Phi_1} = \frac{n_2 V_2}{n_0 v / 4}$$

$n_0$  is the particle density at the shock

The probability of escape is crucial in the determination of the integral energy spectrum

$$N(> E) = N_0 \left( \frac{E}{E_0} \right)^{-\gamma} \quad \gamma = \frac{P_{esc}}{\Delta E / E}$$



# Starting from first order Fermi acceleration...

$$P_{esc} = \frac{\Phi_2}{\Phi_1} = \frac{n_2 V_2}{n_0 v / 4} \longrightarrow \gamma = \frac{P_{esc}}{\Delta E / E}$$

Integral energy spectrum index

$$N(> E) = N_0 \left( \frac{E}{E_0} \right)^{-\gamma}$$

## Diffusive shock acceleration

$$n_2 = n_0$$

$$\gamma = \frac{3}{r - 1}$$

r is the compression ratio of the shock

## Superdiffusive shock acceleration (Perri and Zimbardo, ApJ 2012)

$$n(x, E, t) = \int P(x - x', t - t') S_{sh}(x', E, t') dx' dt'$$

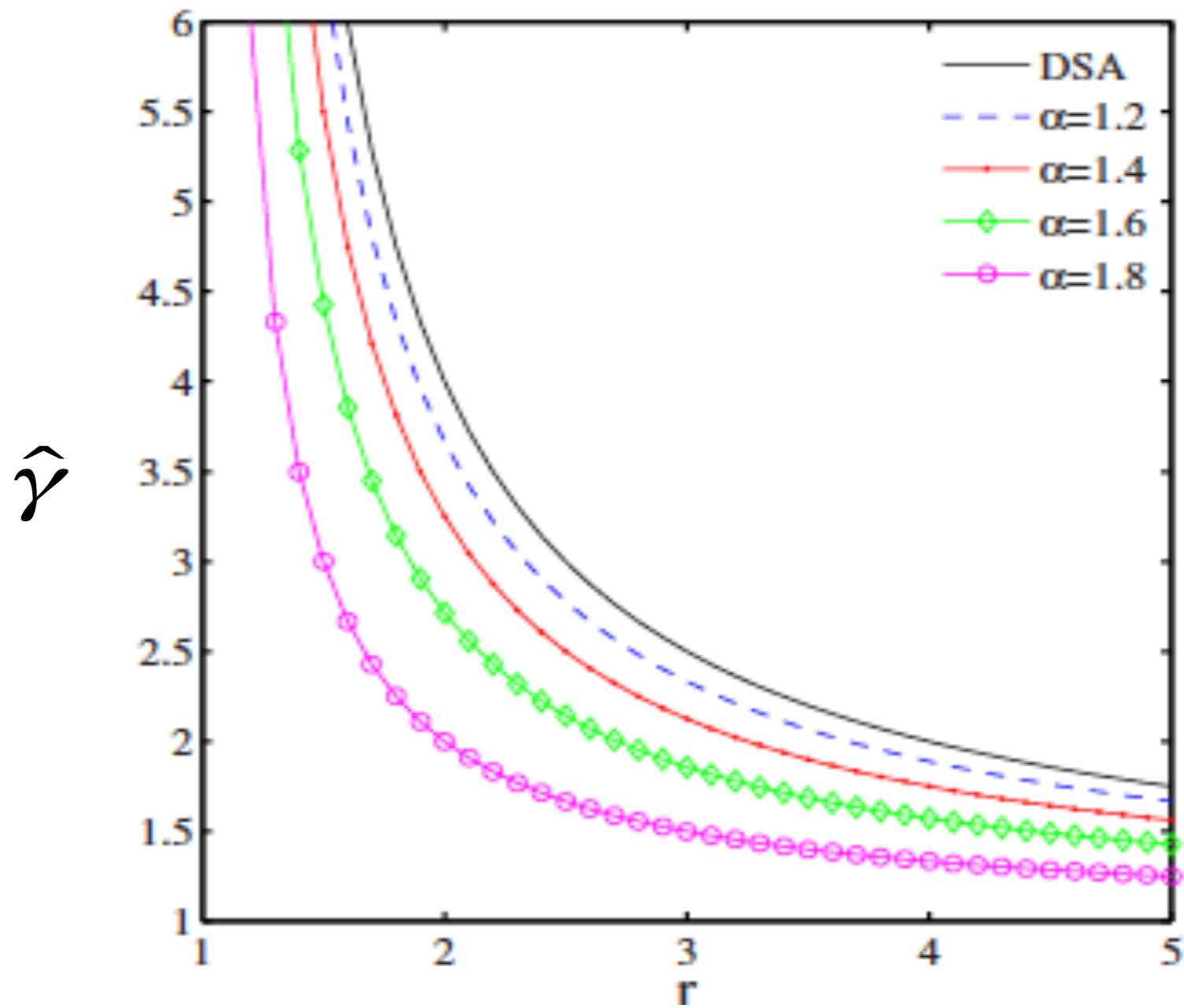
Computing  $n(V_{sh}t, t) = n_0$

In stationary conditions the particle density far downstream is  $n_2 = \Phi_0 / V_{sh}$

$$\frac{n_2}{n_0} = 2 \frac{\mu - 2}{\mu - 1} = 2 \frac{2 - \alpha}{3 - \alpha}$$

$$\langle \Delta r^2 \rangle = 2D_\alpha t^\alpha$$

$$\gamma = \frac{P_{esc}}{\Delta E / E} = 6 \frac{2 - \alpha}{3 - \alpha} \frac{1}{r - 1}$$



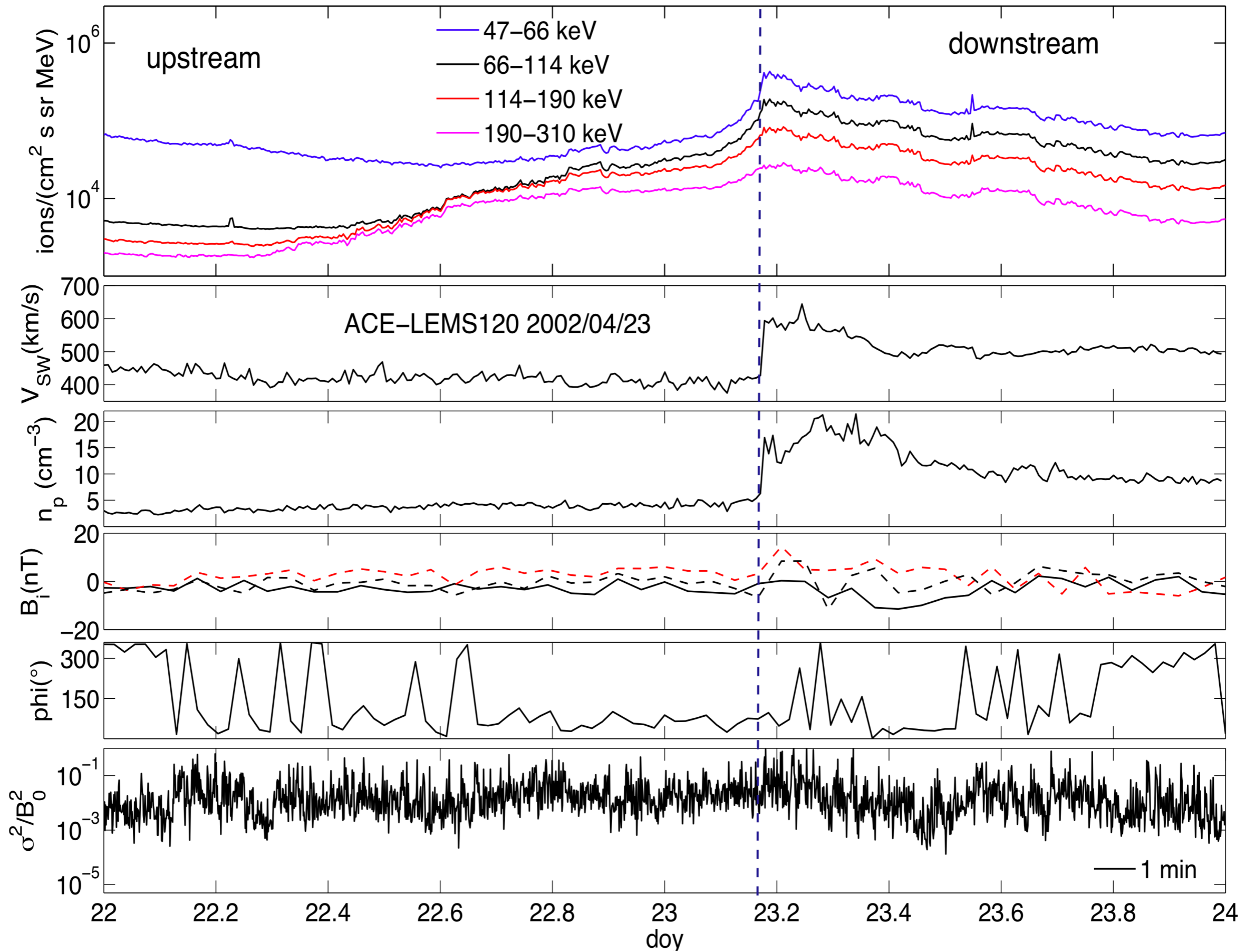
Differential energy spectral index

$$\hat{\gamma} = \gamma + 1$$

$$\hat{\gamma}^{DSA} = \frac{r + 2}{r - 1}$$

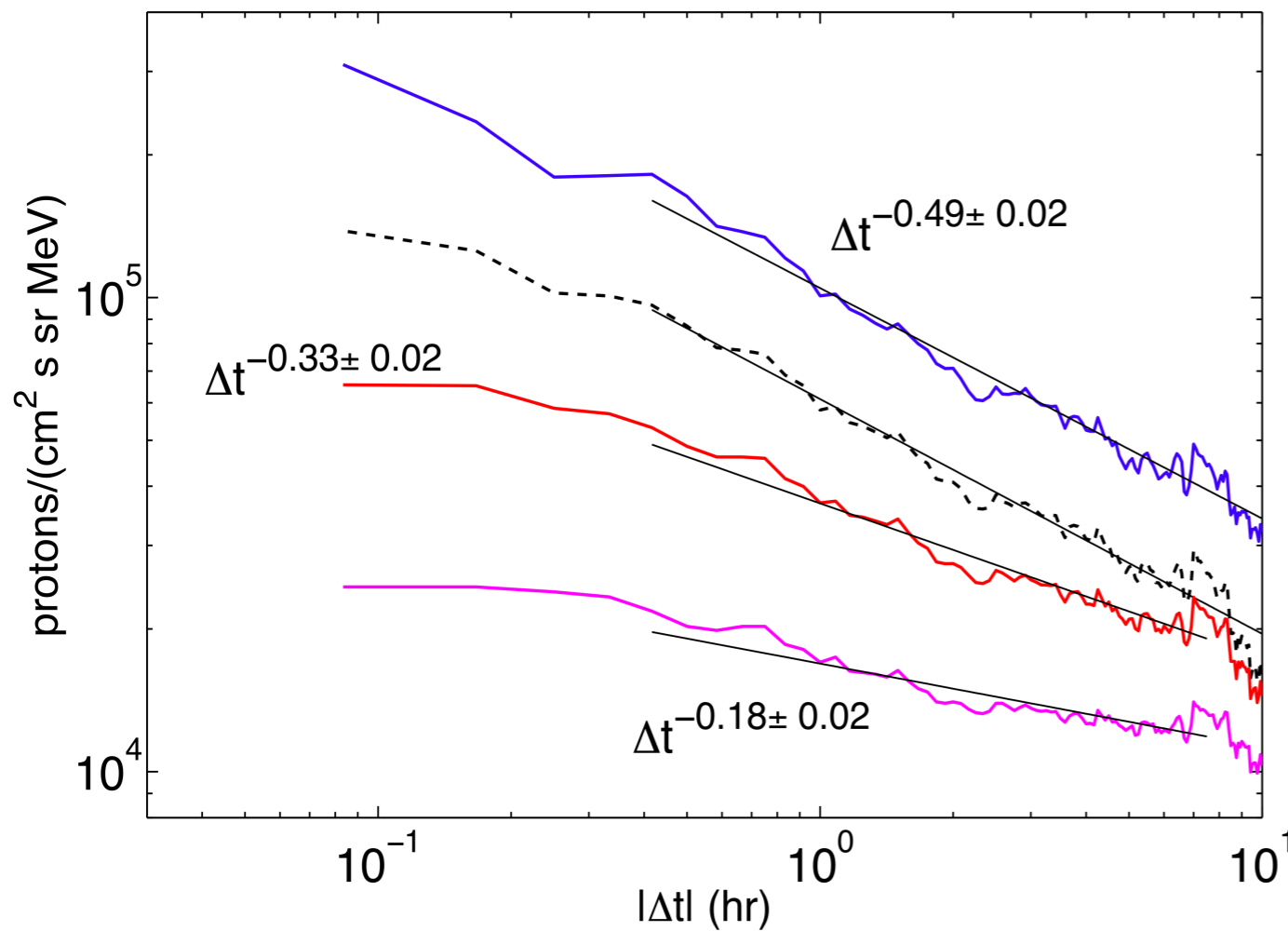
$$\hat{\gamma}^{SSA} = \frac{6}{r - 1} \left( \frac{2 - \alpha}{3 - \alpha} \right) + 1$$

**Energy spectral indices harder than those predicted by DSA**



ACE data

ACE-LEMS120, 2002 doy 113



$$\Delta t = |t - t_{sh}|$$

The energy spectrum is in a better agreement with the SSA prediction (more events shown in *Perri et al., 2015*)

Superdiffusive protons

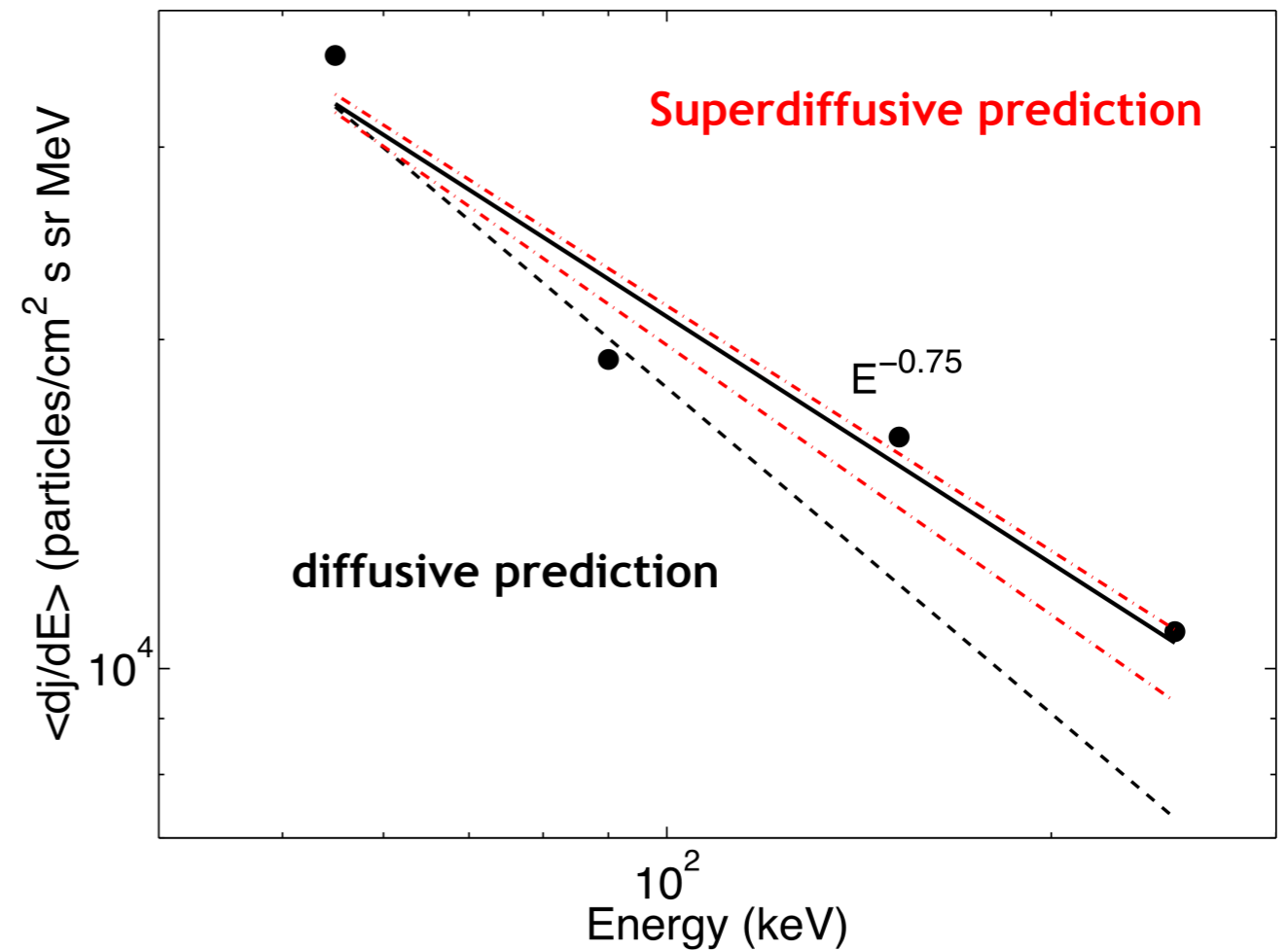
$$n(\Delta t, E) \propto |\Delta t|^{-\beta}$$

$$|x| = V_{sh} \Delta t$$

$$\langle \Delta x^2(t) \rangle \propto t^{2-\beta}$$

$$2 - \beta \in [1.51, 1.82]$$

ACE-LEMS120 23/04/2002-upstream



# Acceleration time

## DSA

$$t_{cycle}^D = \frac{4}{v} \left( \frac{D_1}{V_1} + \frac{D_2}{V_2} \right)$$

time to cross the shock from upstream to downstream and back

$$t_{acc}^D = \frac{t_{cycle}^D}{\Delta E / E} = \frac{3}{V_1 - V_2} \left( \frac{D_1}{V_1} + \frac{D_2}{V_2} \right)$$

## SSA

Comparing the advective motion to the superdiffusive particle motion

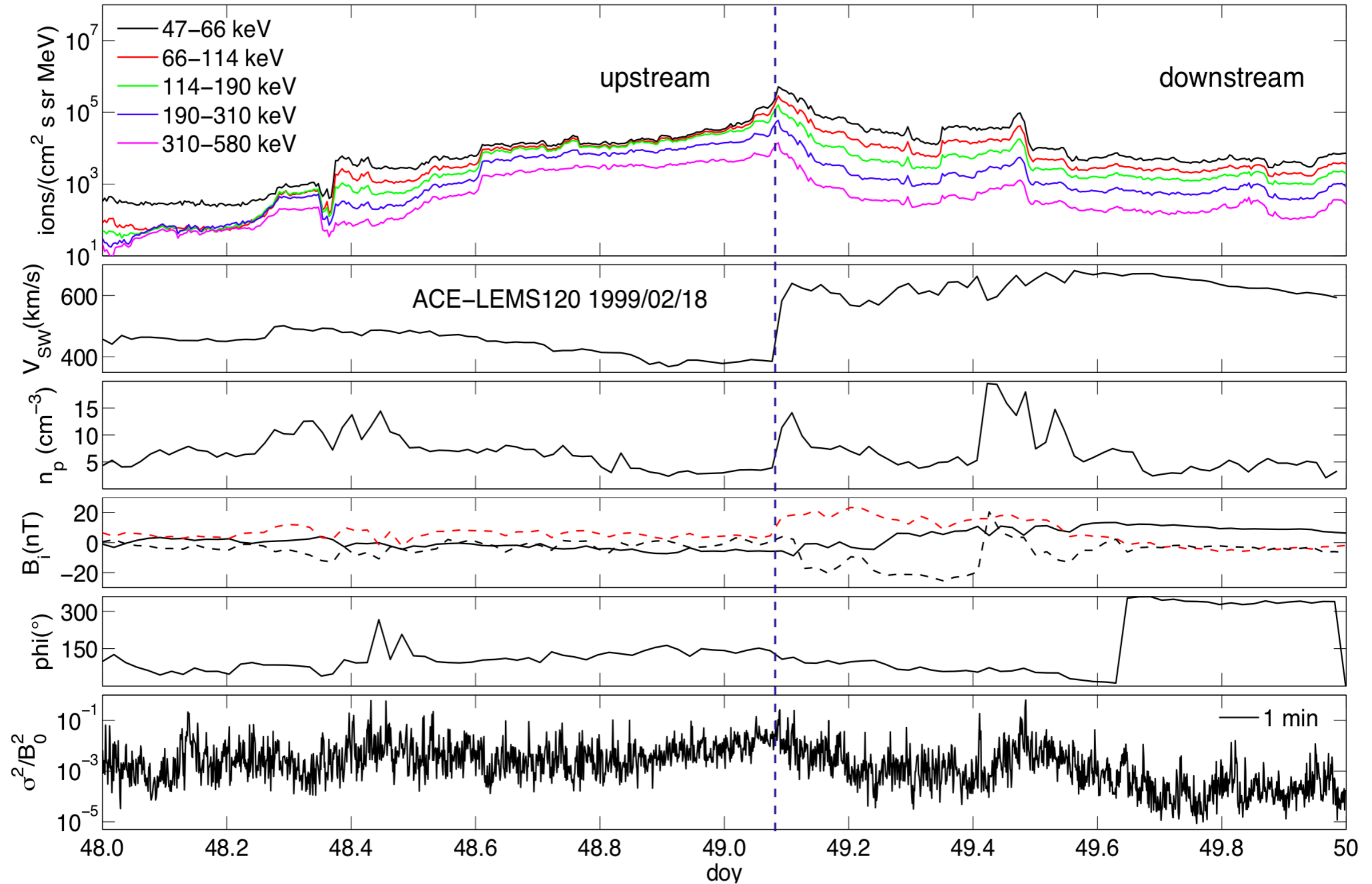
$$\Delta x \approx V \Delta t$$

$$\langle \Delta x^2 \rangle = 2D_\alpha t^\alpha$$

$$t_{acc}^S = \frac{3}{V_1 - V_2} \left[ \left( \frac{D_{\alpha 1}}{V_1^\alpha} \right)^{1/(2-\alpha)} + \left( \frac{D_{\alpha 2}}{V_2^\alpha} \right)^{1/(2-\alpha)} \right]$$

This will be estimated from data analysis

# Estimation of acceleration time



## ACE observations

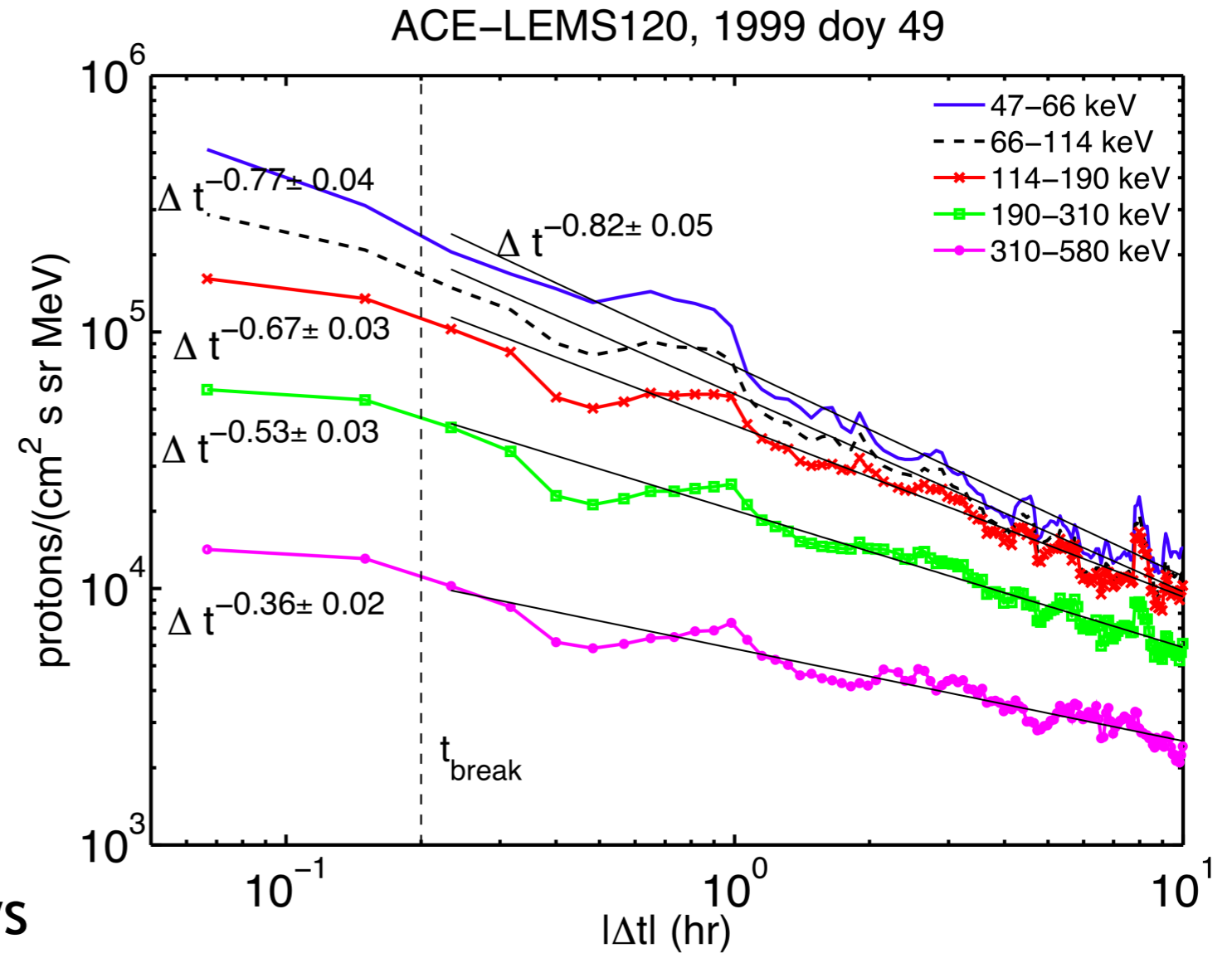
Perri and Zimbardo, *J. Phys. Conf. Ser.*, 2015

$$t_{acc}^S = \frac{3}{V_1 - V_2} \left[ \left( \frac{D_{\alpha 1}}{V_1^\alpha} \right)^{1/(2-\alpha)} + \left( \frac{D_{\alpha 2}}{V_2^\alpha} \right)^{1/(2-\alpha)} \right]$$

In the framework of superdiffusion, the propagator has different shapes close to the source and far from the source (*Zumofen and Klafter, 1993*).

From s/c observations a time  $t_{\text{break}}$  at which the particle profile changes can be determined

*Perri et al., Astron. Astrophys. 2015* have shown that  $t_{\text{break}}$  allows to estimate the anomalous diffusion coefficient for particle at a given energy



*Perri and Zimbardo, J. Phys. Conf. Ser., 2015*

$$t_{acc}^D = \frac{3}{V_1 - V_2} \left( \frac{D_1}{V_1} + \frac{D_2}{V_2} \right)$$

$$D = \frac{1}{3} \lambda v \longrightarrow \lambda = 0.1 \text{ AU}$$

$$D_2 = \frac{D_1}{r}$$

$$t_{acc}^S = \frac{3}{V_1 - V_2} \left[ \left( \frac{D_{\alpha 1}}{V_1^\alpha} \right)^{1/(2-\alpha)} + \left( \frac{D_{\alpha 2}}{V_2^\alpha} \right)^{1/(2-\alpha)} \right]$$

$$D_{\alpha 2} = \frac{D_{\alpha 1}}{r}$$

*Perri and Zimbardo, Astrophys. J., 2015*

## 1999/02/18-ACE

$V_{sh}$ (km/s)	$V_1$ (km/s)	$V_2$ (km/s)	$\theta_{Bn}$ ( $^\circ$ )	$E_K$ (keV)	$\alpha$	$t^S$ (days)	$t^D$ (days)
759	380	180	63	47-66	1.18	0.5	3
				66-114	1.23	0.5	4
				114-190	1.33	0.4	5
				190-310	1.47	0.5	7
				310-580	1.64	0.8	7

**Shorter acceleration times when superdiffusion is taken into account. They are compatible with the lifetime of the system.**



# A Lévy random walk test particle model

Prete et al., Adv. Space Res., 2019

A Langevin type equation for particles is integrated

$$dx_i = V_{\text{bulk}} dt_i + v_{\text{random}} dt_i$$

$$n(x) = \Phi_0 \int_0^\infty P(x, t) dt$$

**Diffusion**

$$P(x, t) = \frac{1}{\sqrt{4\pi Dt}} \exp[-(x - V_{\text{bulk}}t)^2 / 4Dt]$$

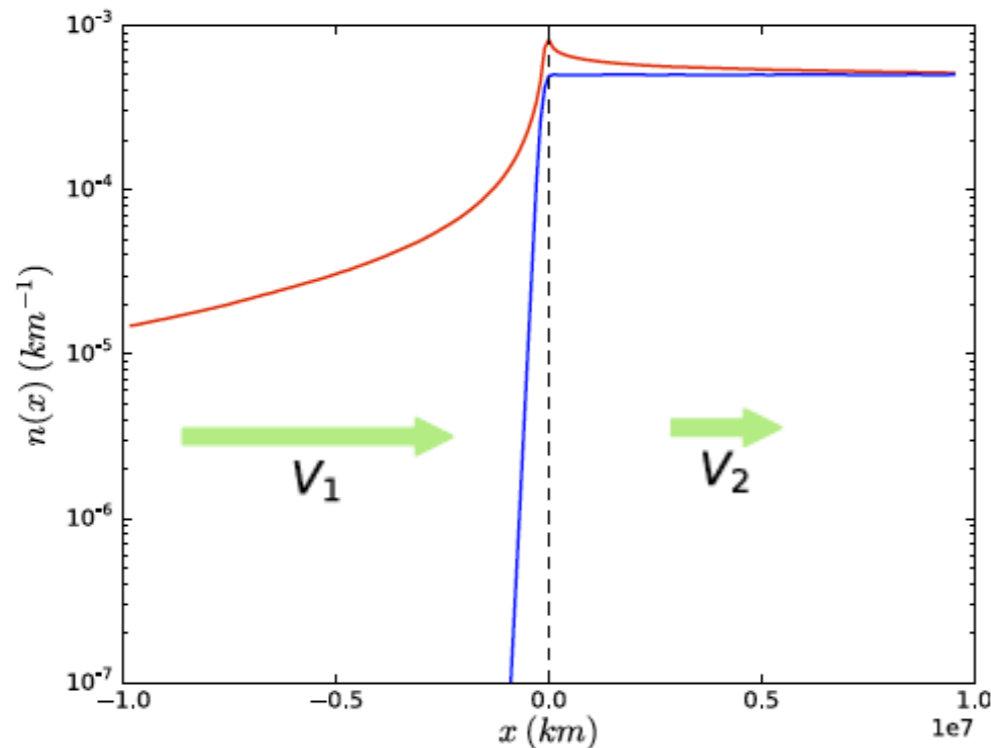


Fig. 10. This figure shows a direct comparison between the density profiles obtained in the diffusive case (blue line,  $\tau = 50$  s) and the superdiffusive case (red line,  $\mu = 2.5$ ,  $\tau_0 = 50$  s). (For interpretation of the

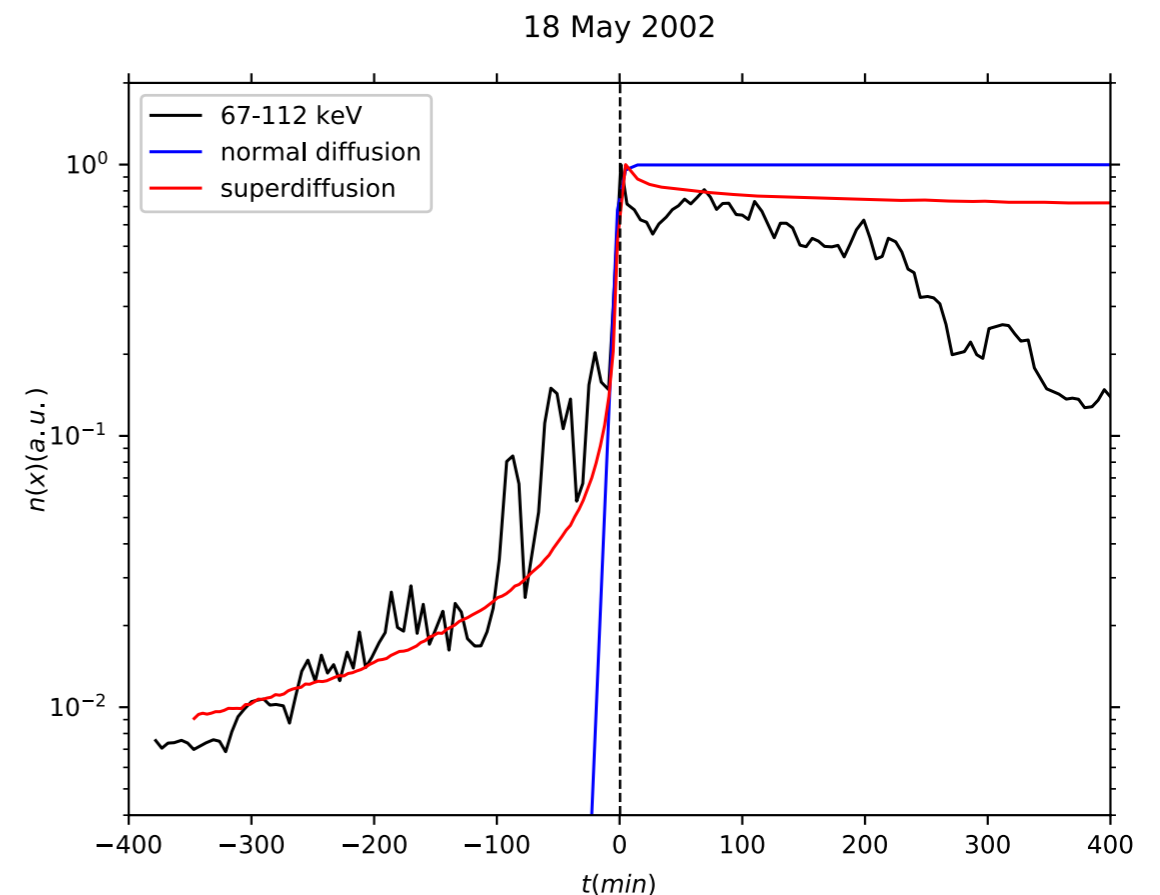
**Superdiffusion**

Distribution of free-path length

$$\Psi(\ell, \tau) = \begin{cases} \frac{1}{2} C \delta(|\ell| - v\tau), & |\ell| < \ell_0 \\ \frac{1}{2} C |\ell/\ell_0|^{-\mu} \delta(|\ell| - v\tau), & |\ell| > \ell_0. \end{cases}$$

$$\tau = \tau_0 \left[ \frac{1}{\mu(1 - \xi)} \right]^{\frac{1}{\mu-1}}$$

Power law distribution of scattering time



# Superdiffusive transport at SNRs

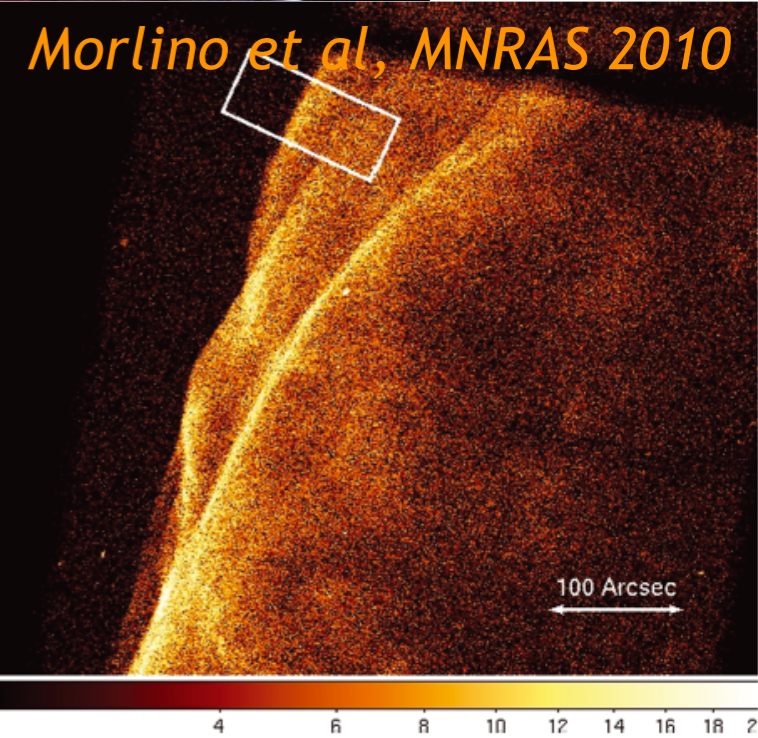
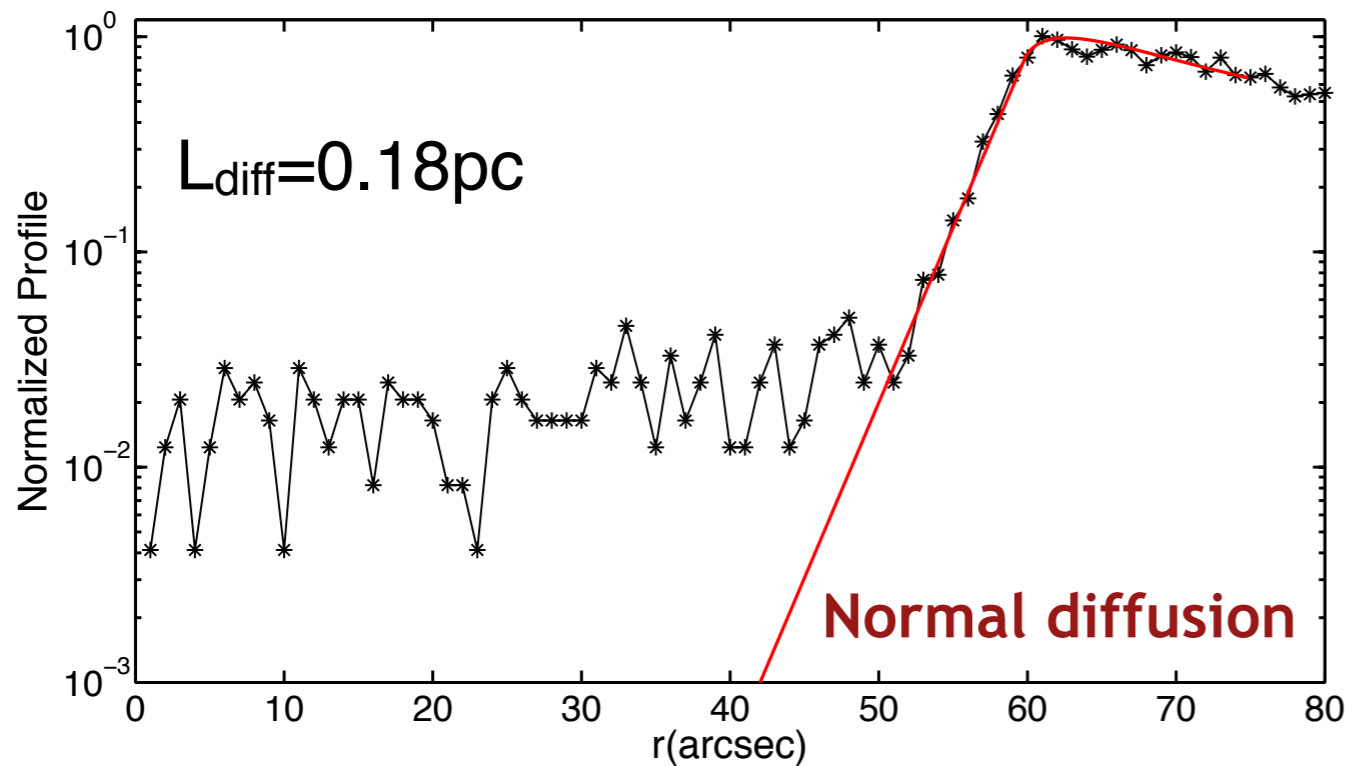


**Figure 1.** *Chandra* X-ray image of the north-eastern limb showed in squared root colour scale. The white rectangle ( $50 \times 120 \text{ arcsec}^2$ ) is the region used

SN1006 X-Ray Profile 1keV



$$B_1 = B_2/\sqrt{11} = 11 \mu\text{G}, \quad \text{for a strong shock}$$

downstream:

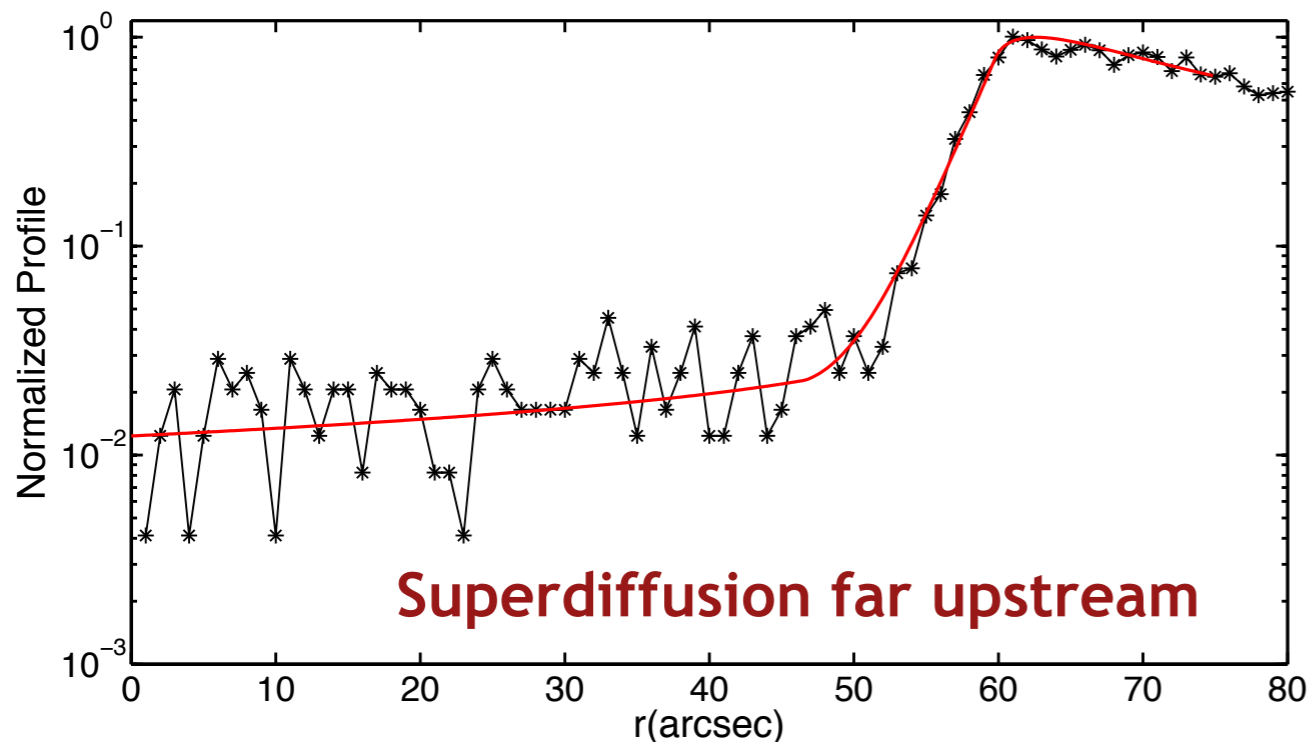
$$f_{e,2}(E, x) = f_0 \exp(-x/\Delta R_2),$$

$$\Delta R_2 = \frac{V_2 \tau_{\text{syn}}}{2} \left[ 1 + \sqrt{\left( 1 + \frac{4D_2}{V_2^2 \tau_{\text{syn}}} \right)} \right]$$

upstream (balance between advection and diffusion):

$$f_{e,1}(E, x) = f_0 \exp(V_1 x/D_1)$$

SN1006 X-Ray Profile 1keV



upstream (balance between advection and super diffusion far upstream):

$$f_e(E, x) = f_0 \exp(-V_1|x|/D_1), \quad 0 < |x| < L_{\text{prec}}$$

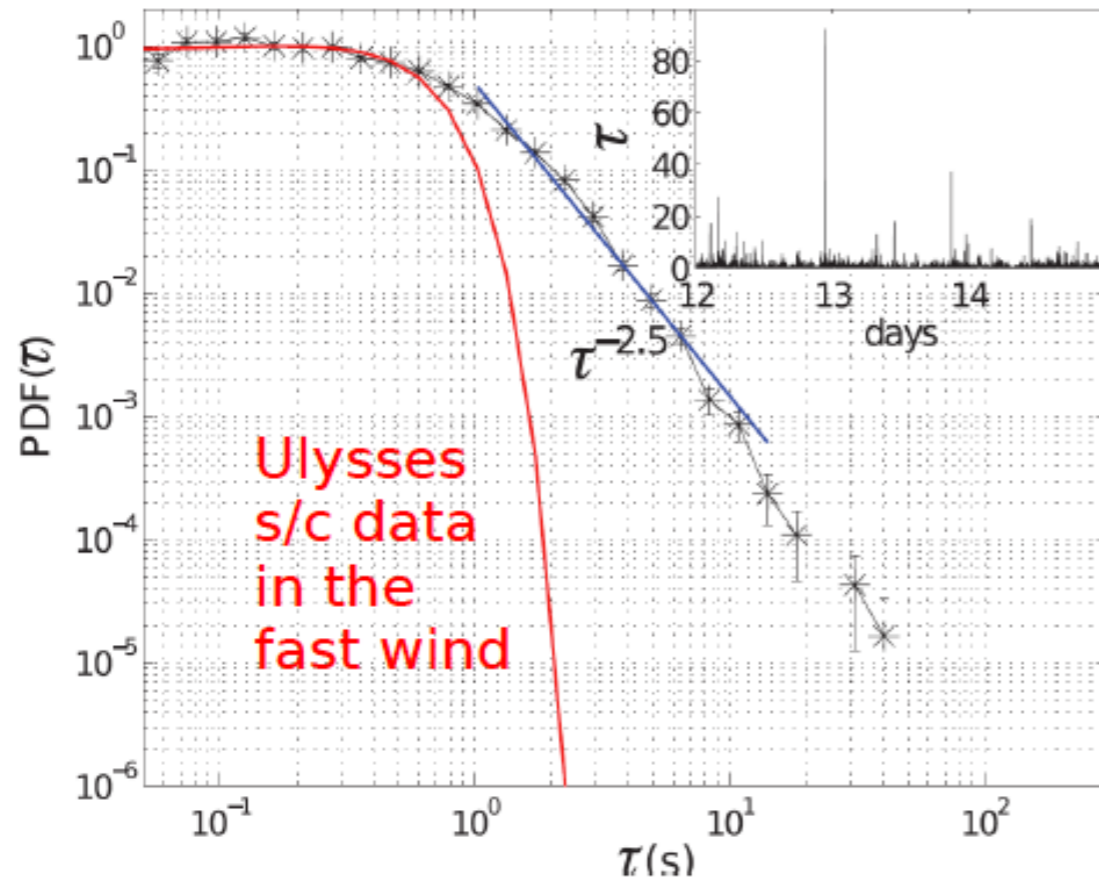
$$f_e(E, x) = f_0 \exp(-V_1 L_{\text{prec}}/D_1) \frac{L_{\text{prec}}^a}{|x|^a}, \quad |x| > L_{\text{prec}}$$

$$L_{\text{prec}} = 0.85 \text{ pc}, \quad a = 0.7$$

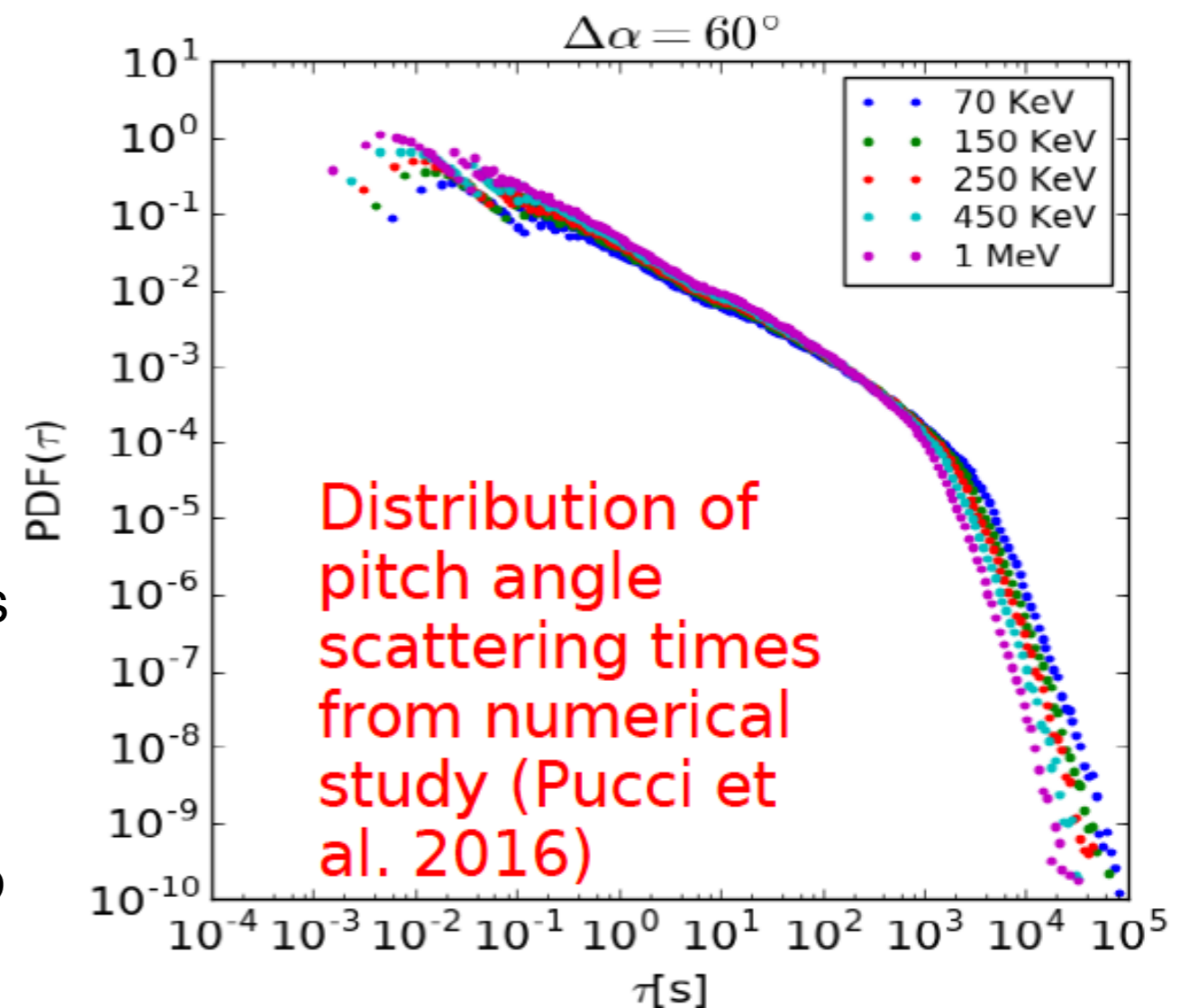
$$L_{\text{diff}}(300 \text{ TeV}) = 0.7 \text{ pc}$$

# On the possible origin of superdiffusion

– Perri and Zimbardo, *Astrophys. J. Lett.*, 2012  
1995 days 12–15



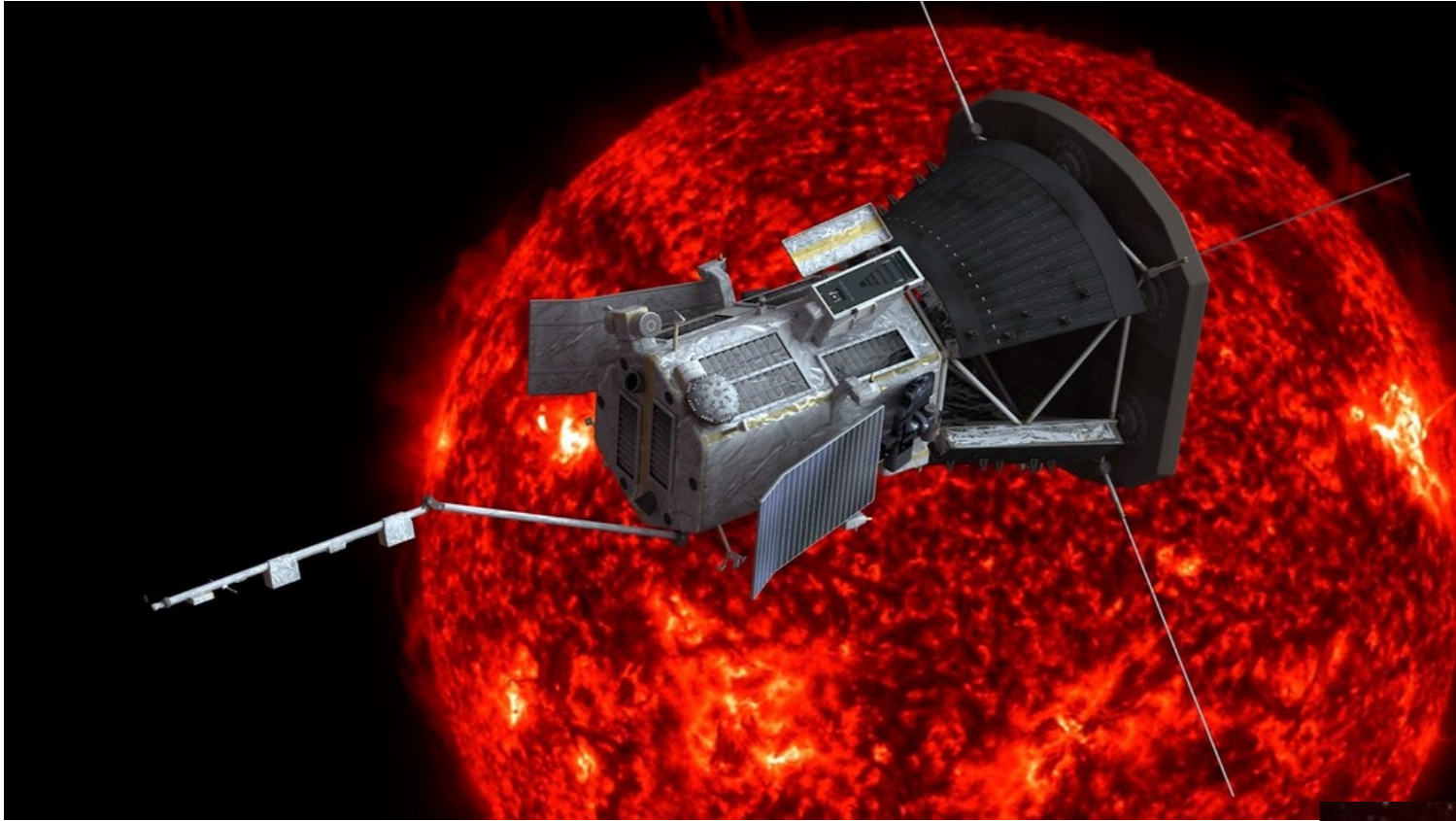
Superdiffusion is due to a stochastic process (Lèvy walk) that is characterized by a power-law distribution of the free path lengths and by a diverging mean free path



- i) probability of occurrence for long displacement higher than a Gaussian;
- ii) very short displacements have also an associated high probability;
- iii) such a scale-free nature of the walk allows particles to make both very long and very short jumps, increasing their probability of returning to the shock (if far away) and crossing the shock several time (if close to the front)

# Outlook

New in-situ measurements from *Parker Solar Probe* will help to advance our knowledge on the particle transport close to source regions



Being close to the source of acceleration, it will be possible to separate the energetic particle "seed" population without any mixing due to effects of propagation in the heliosphere.

Higher resolution data (few seconds) will allow us to better resolve particle fluxes close to the shock front

Thanks to the joint combination between in-situ (as the MAG, SWA, EPD) and remote sensing (EUI, METIS) instruments on board *Solar Orbiter* and to its vicinity to the Sun, we will have the opportunity to study, with unprecedented precision, the onset of Coronal Mass Ejections and the properties of the induced shocks propagating in the interplanetary medium.



# Conclusions

- Several time profiles for particles accelerated at interplanetary shocks decay as power laws with slopes compatible with a superdiffusive transport;
- Superdiffusive Shock Acceleration (SSA) has been developed and directly applied to spacecraft data;
- The acceleration times predicted by SSA for protons accelerated at interplanetary shocks are at least one order of magnitude shorter than the ones obtained from DSA;
- The reduced acceleration time is probably to be ascribed to the scale-free nature of the particle displacements in superdiffusion;
- Superdiffusive transport has also been found by analyzing X-ray intensity radial profiles far upstream of supernova remnant shocks. Close upstream a Bohm diffusion seems to be at work. This combination of regimes explains the steep ramp in the vicinity of the shock and the flat tail far upstream;

- The exponents of superdiffusion found in SNR analysis are consistent with the ones derived from the analysis of upstream energetic particle profiles in the interplanetary space;
- The length at which the X-ray intensity profile changes ( $L_{\text{prec}}$ ) is compatible with the upstream diffusion length of electrons at the highest energy reached in the remnant;
- The new PSP and SO measurements will help us to explore with high resolution energetic particle fluxes accelerated at CMEs driven shocks, allowing to better resolve fluxes close to the shock front. It is fundamental to link the energetic particle transport properties with the plasma turbulence at the relevant scales.